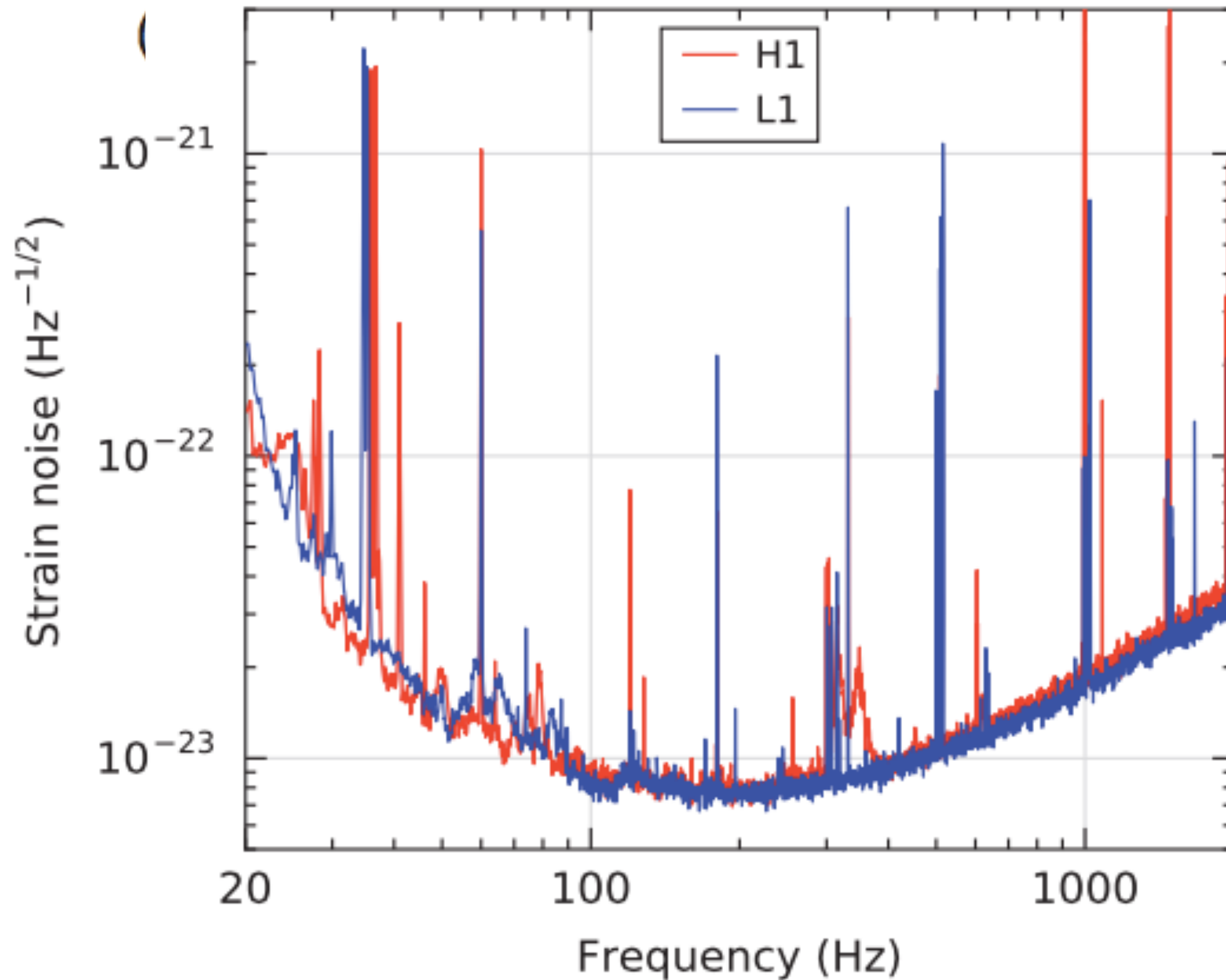


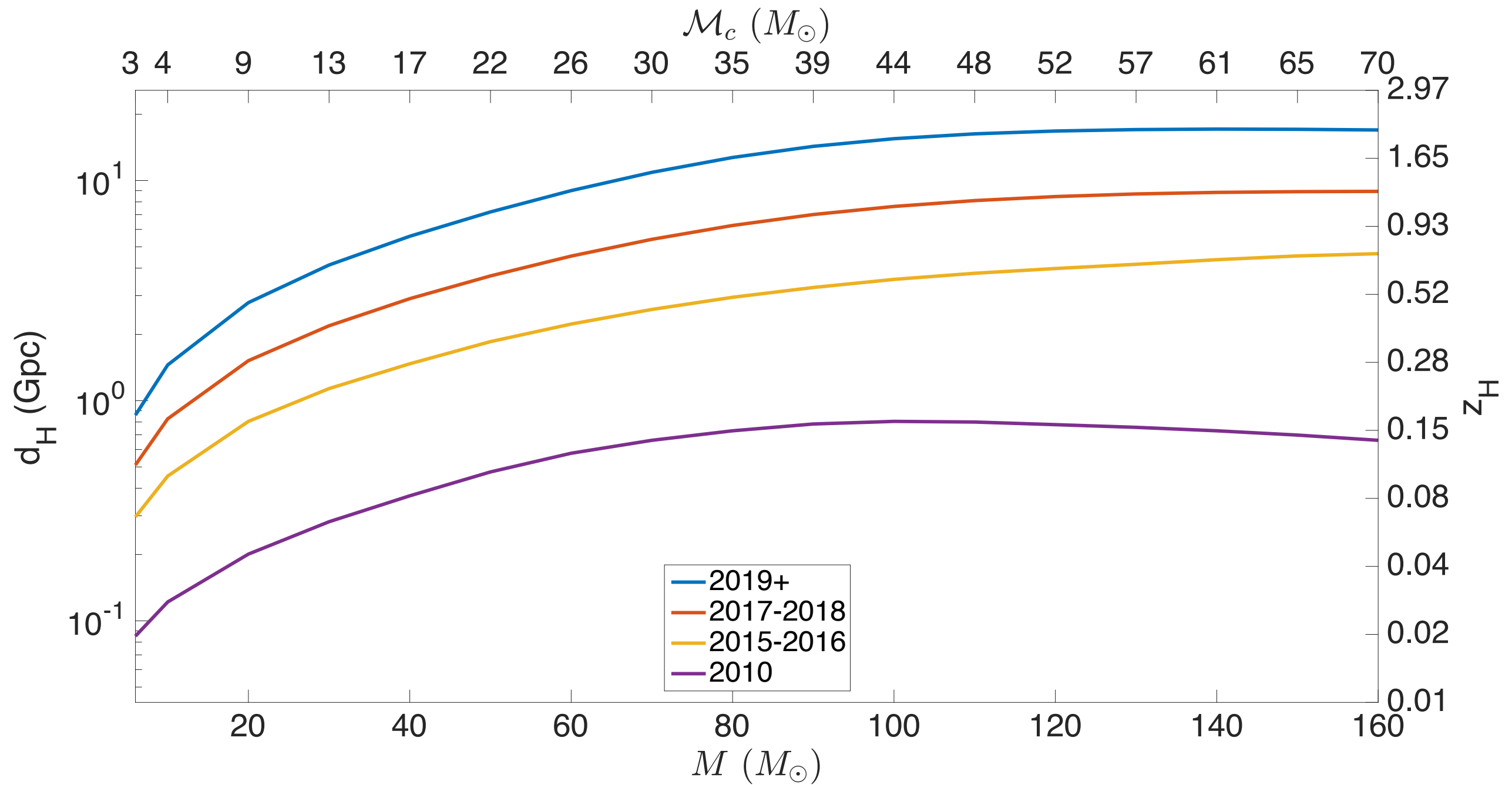
Advanced LIGO noise spectral density

(Abbott et al. PRL 116 (2016) 061102)



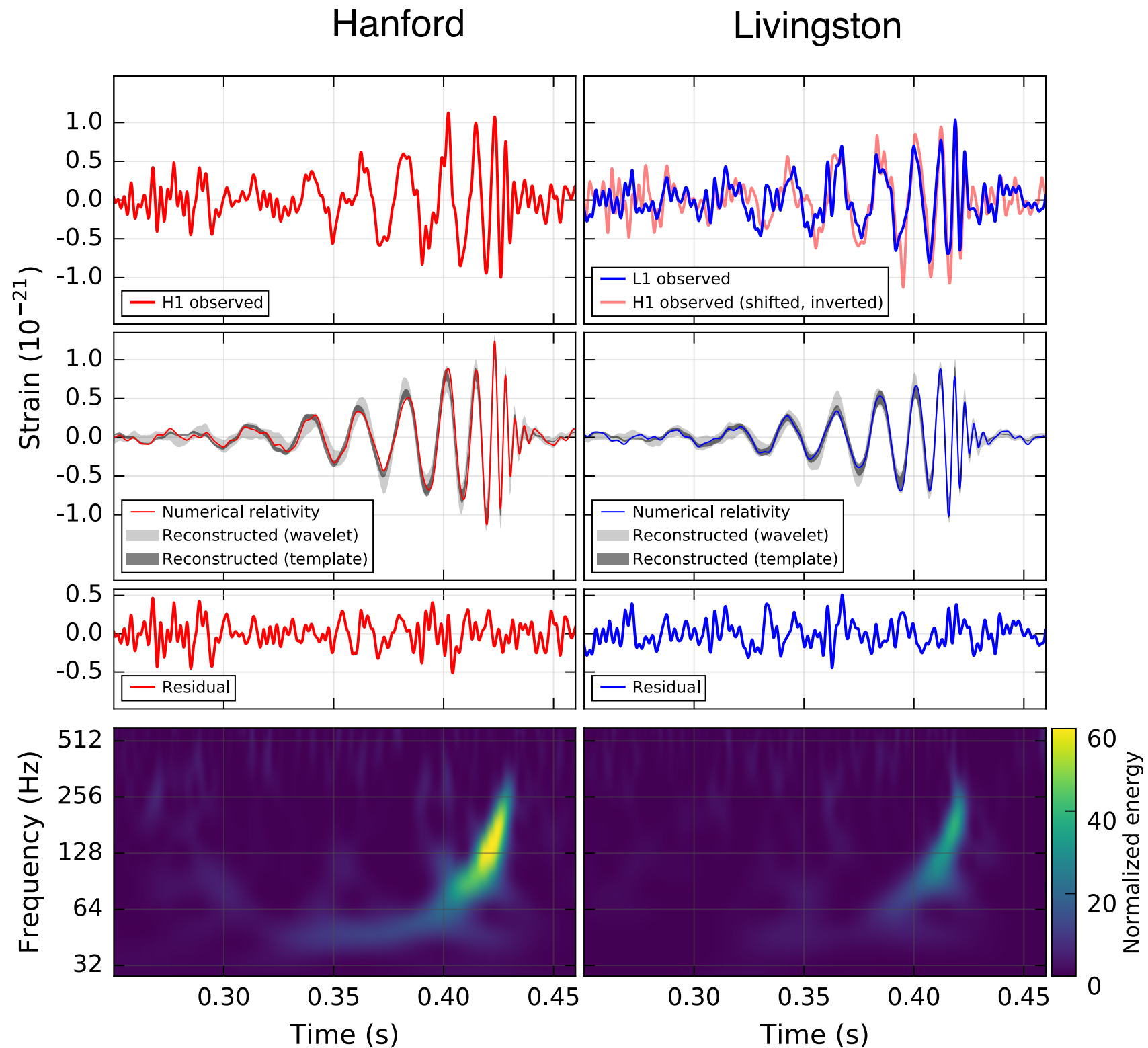
Horizon distance

(Abbott et al. ApJ 818 (2016) no.2, L22)



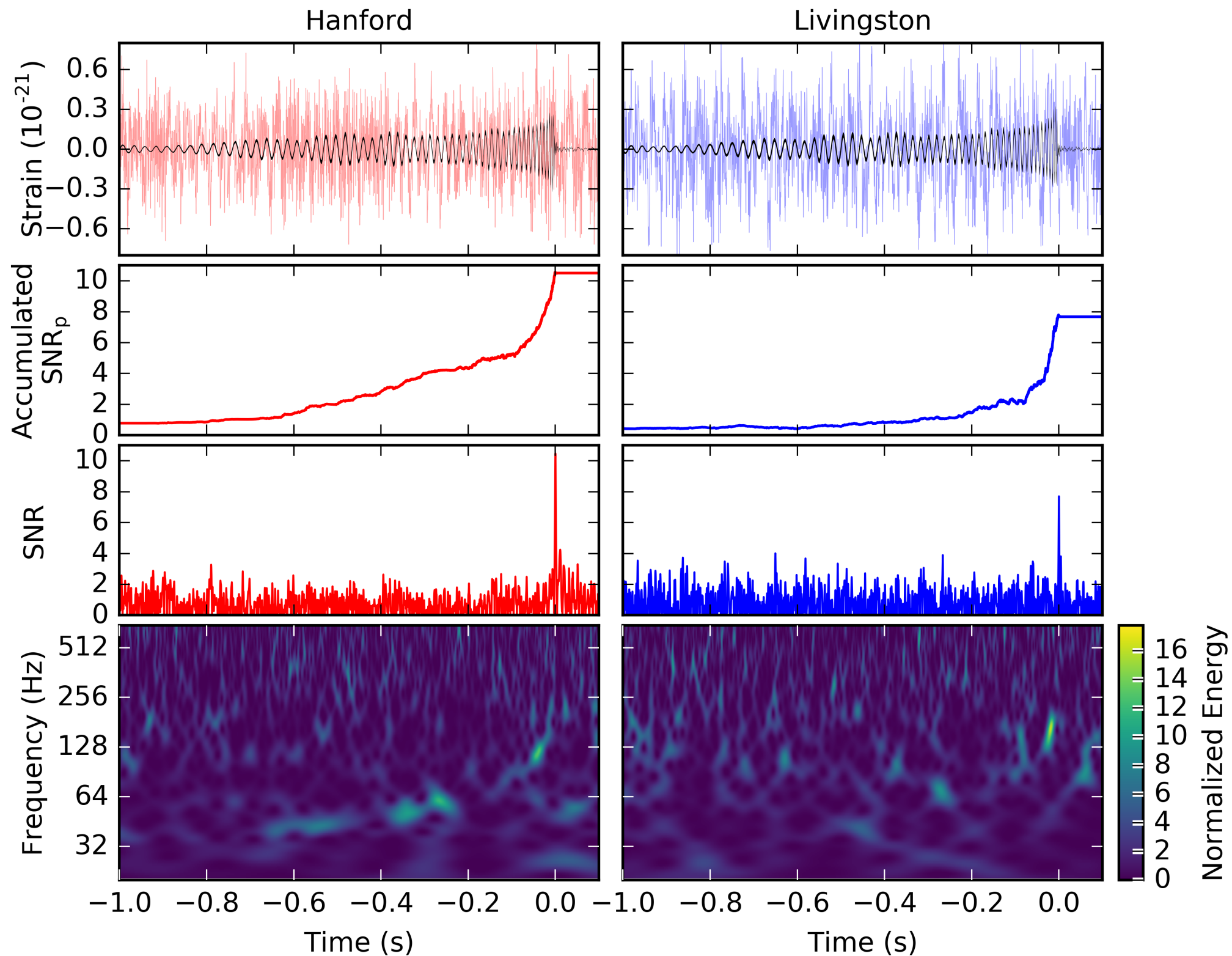
LIGO detections during O1: GW150914

(Abbott et al. PRL 116 (2016) 061102)

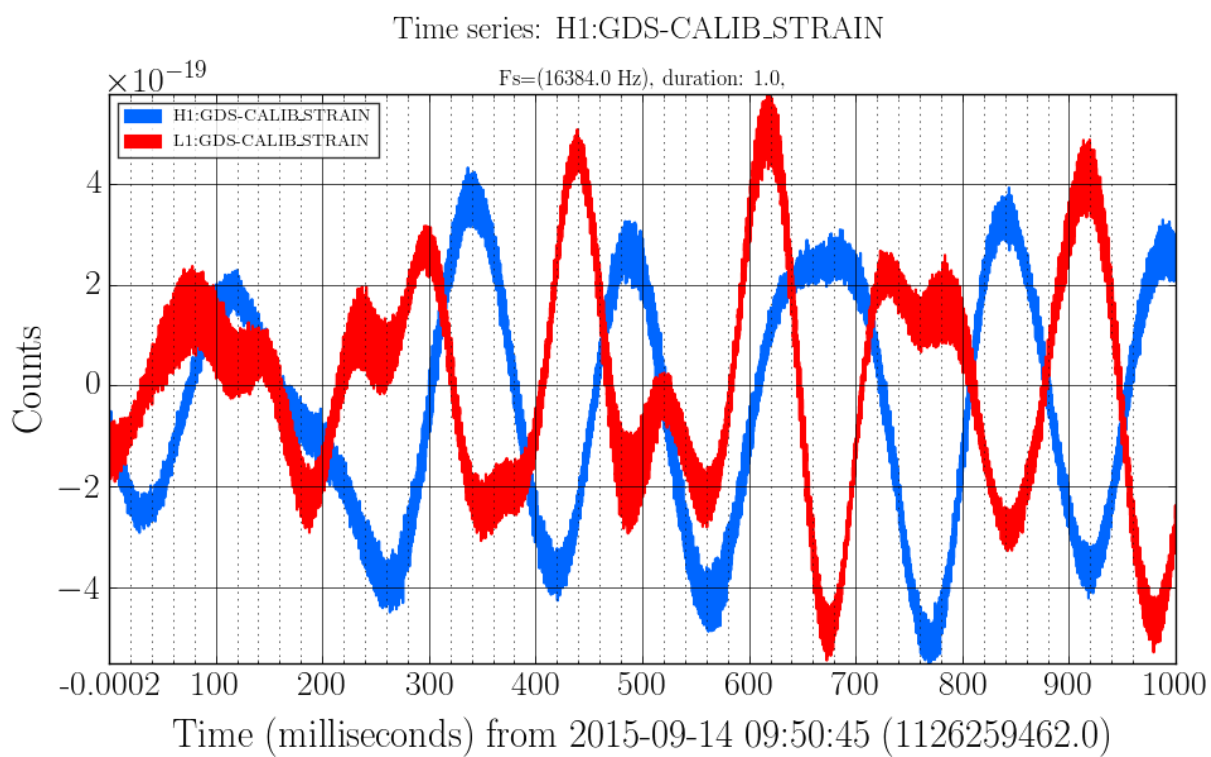


LIGO detections during O1: GW151226

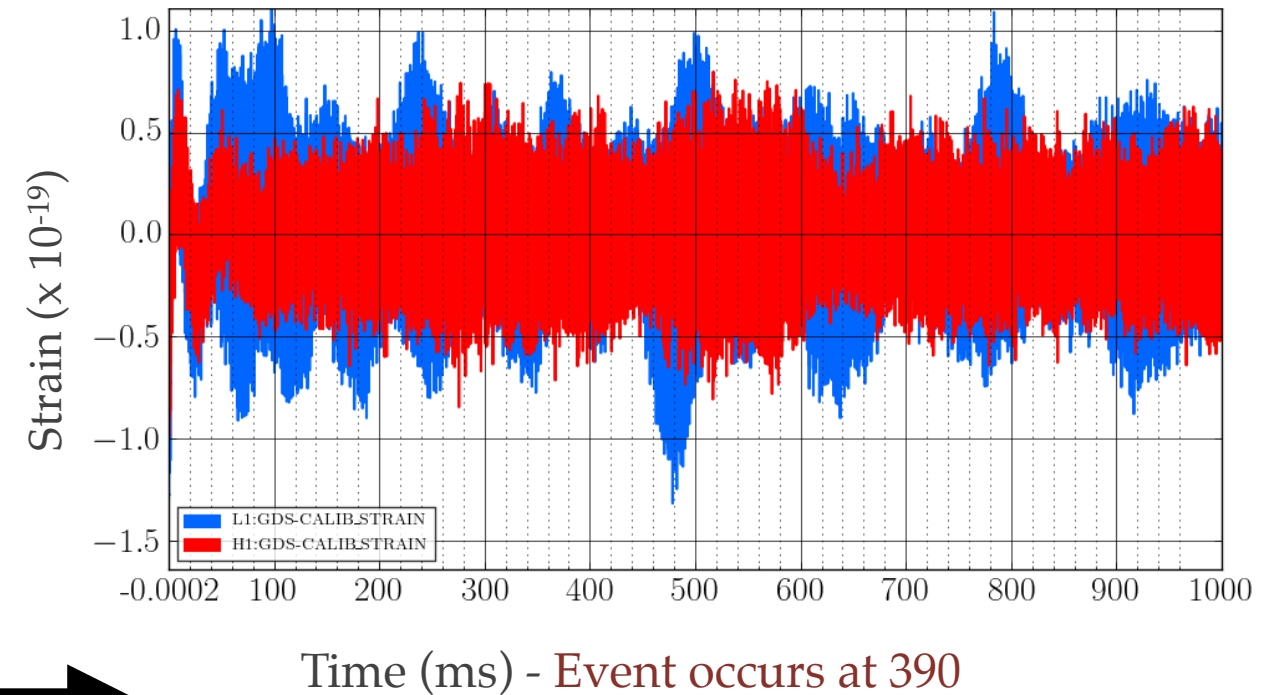
(Abbott et al. PRL 116 (2016) 241103)



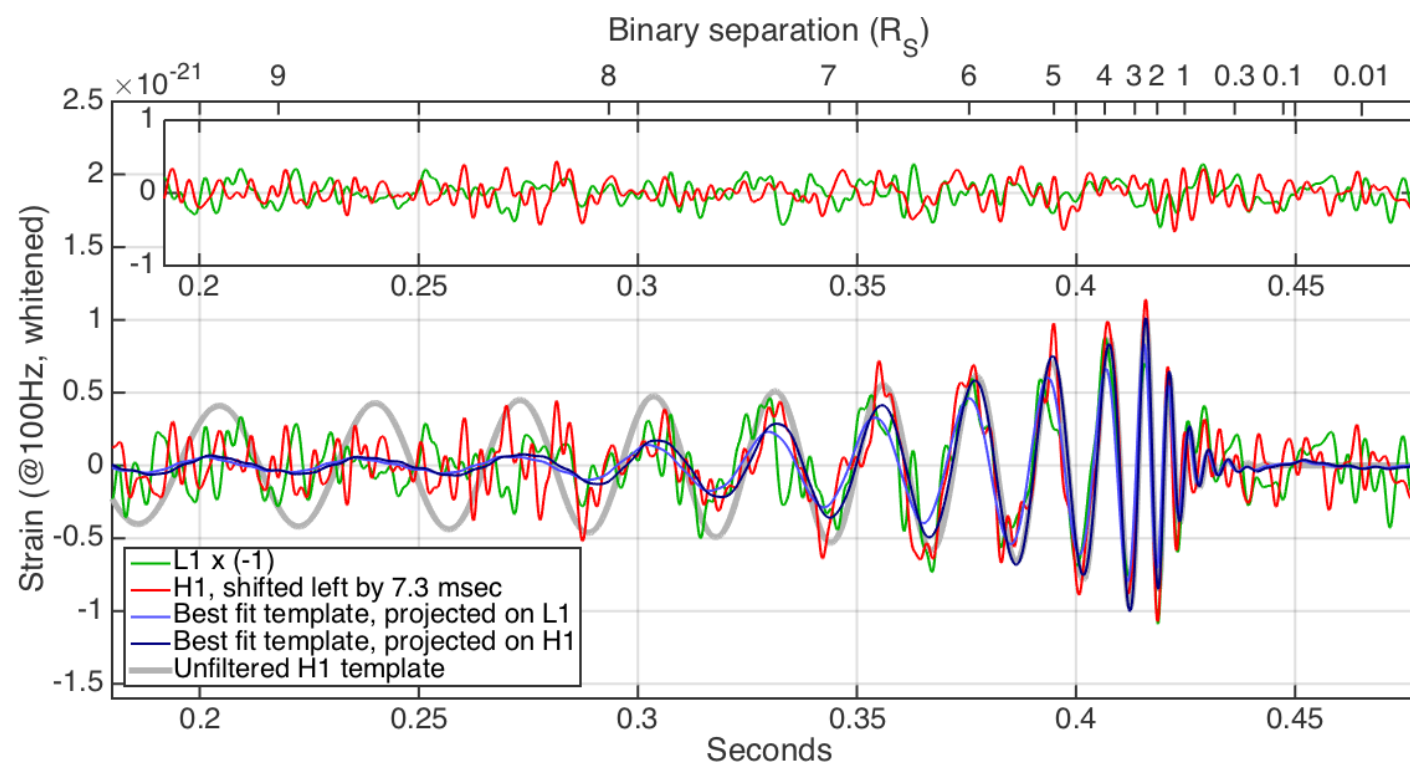
What was originally observed?



(Harry & LIGO Scientific Collaboration)



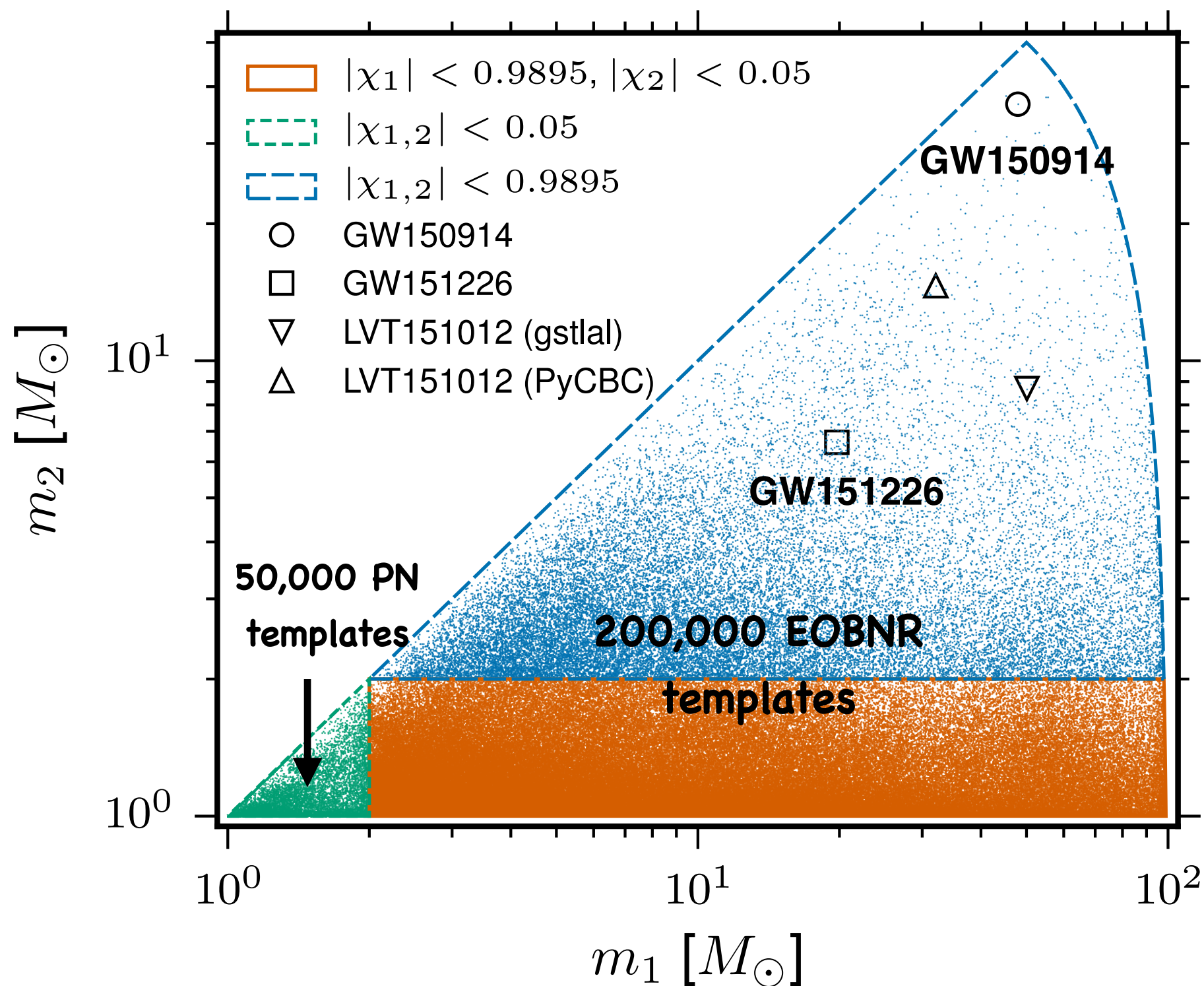
highpass filter



lowpass filter
& whitened

The template bank ("uberbank") for O1

(Abbott et al. arXiv:1606.04856)

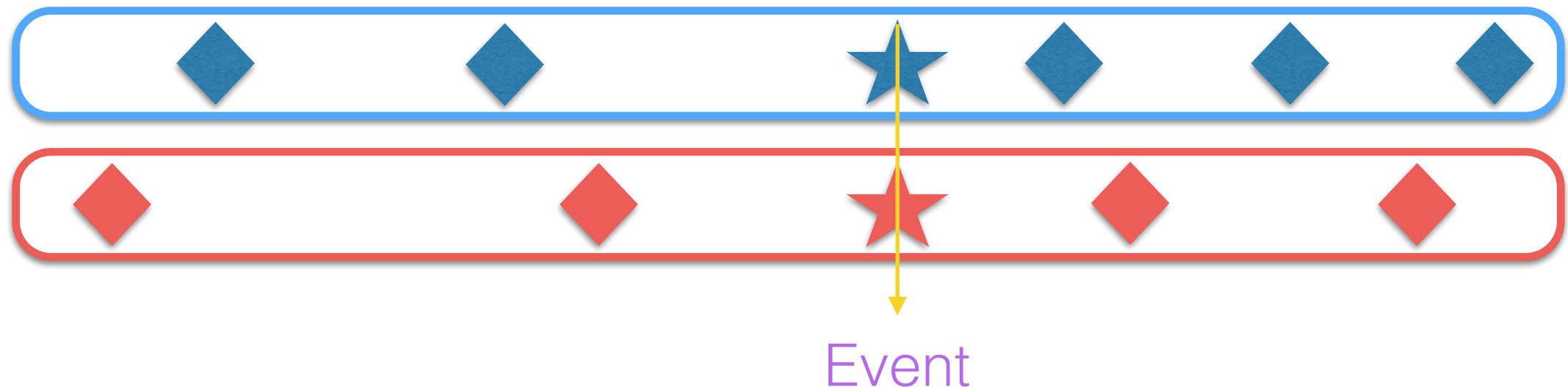


Assessing confidence in LIGO detection

Could the **signal** be **due** to **noise fluctuations**?

(animation by Nuttall)

Zero-lag

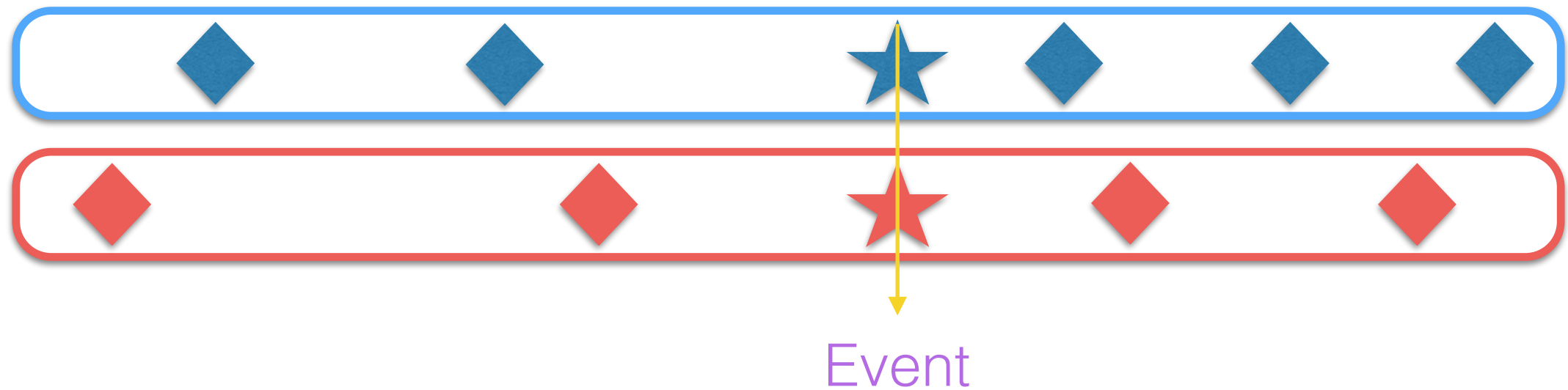


Assessing confidence in LIGO detection

Building larger background by time-shifting the data

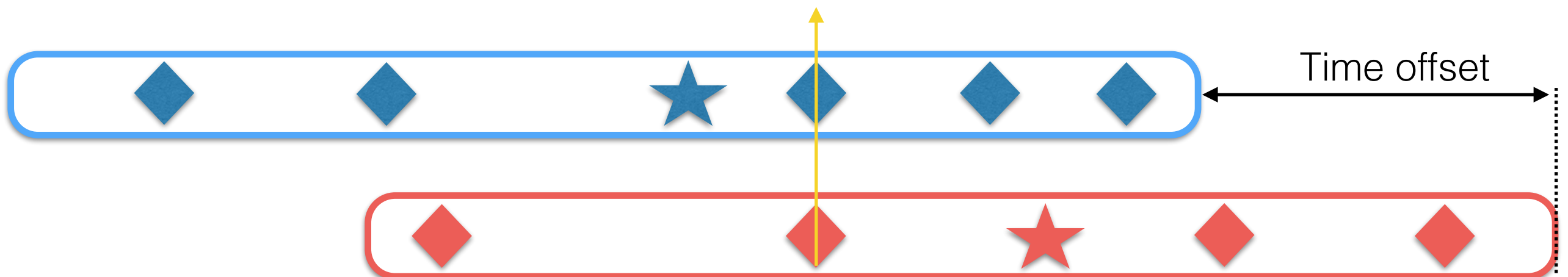
(animation by Nuttall)

Zero-lag



Time slide

Background event

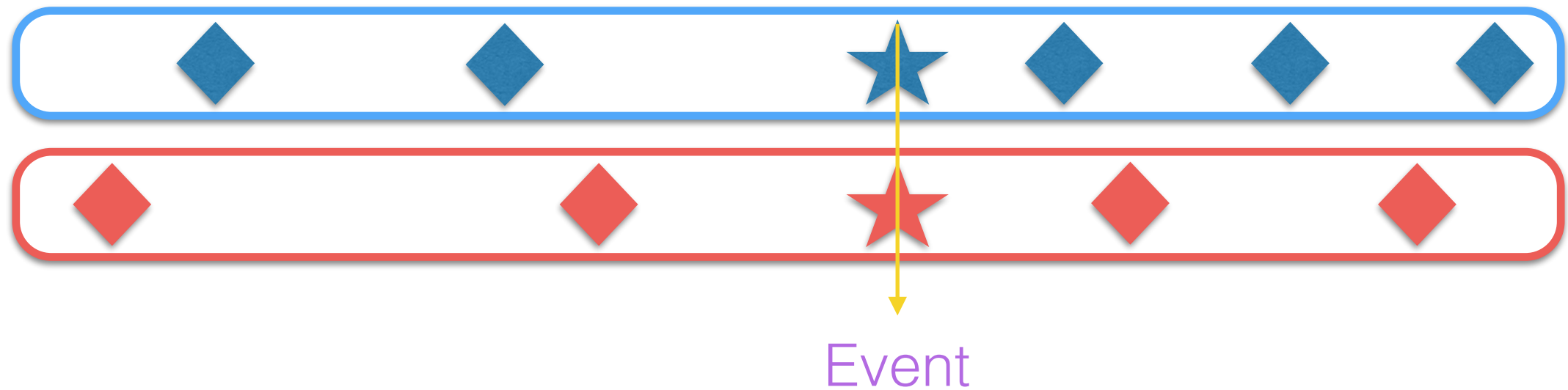


Assessing confidence in LIGO detection

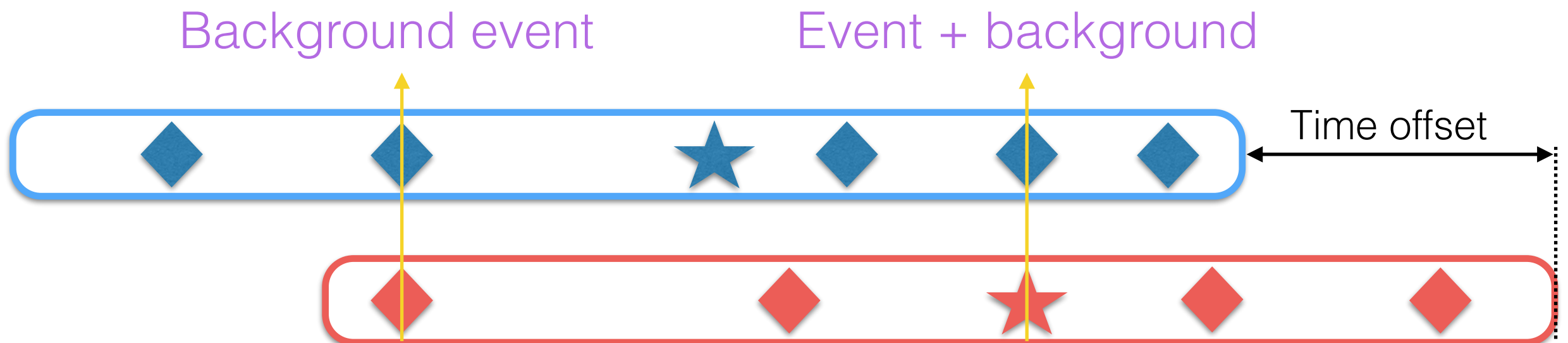
Building larger background by time-shifting the data

(animation by Nuttall)

Zero-lag

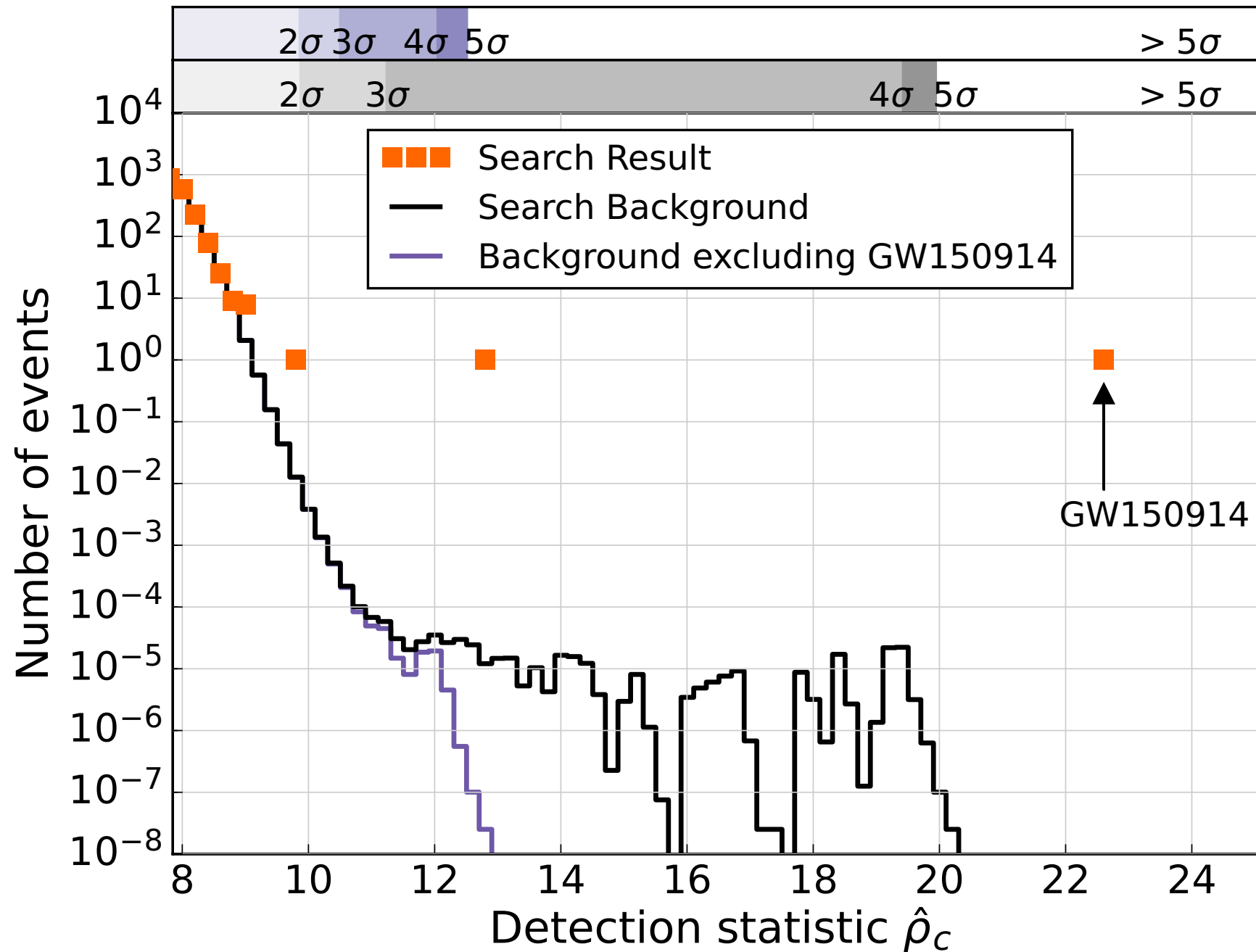


Time slide



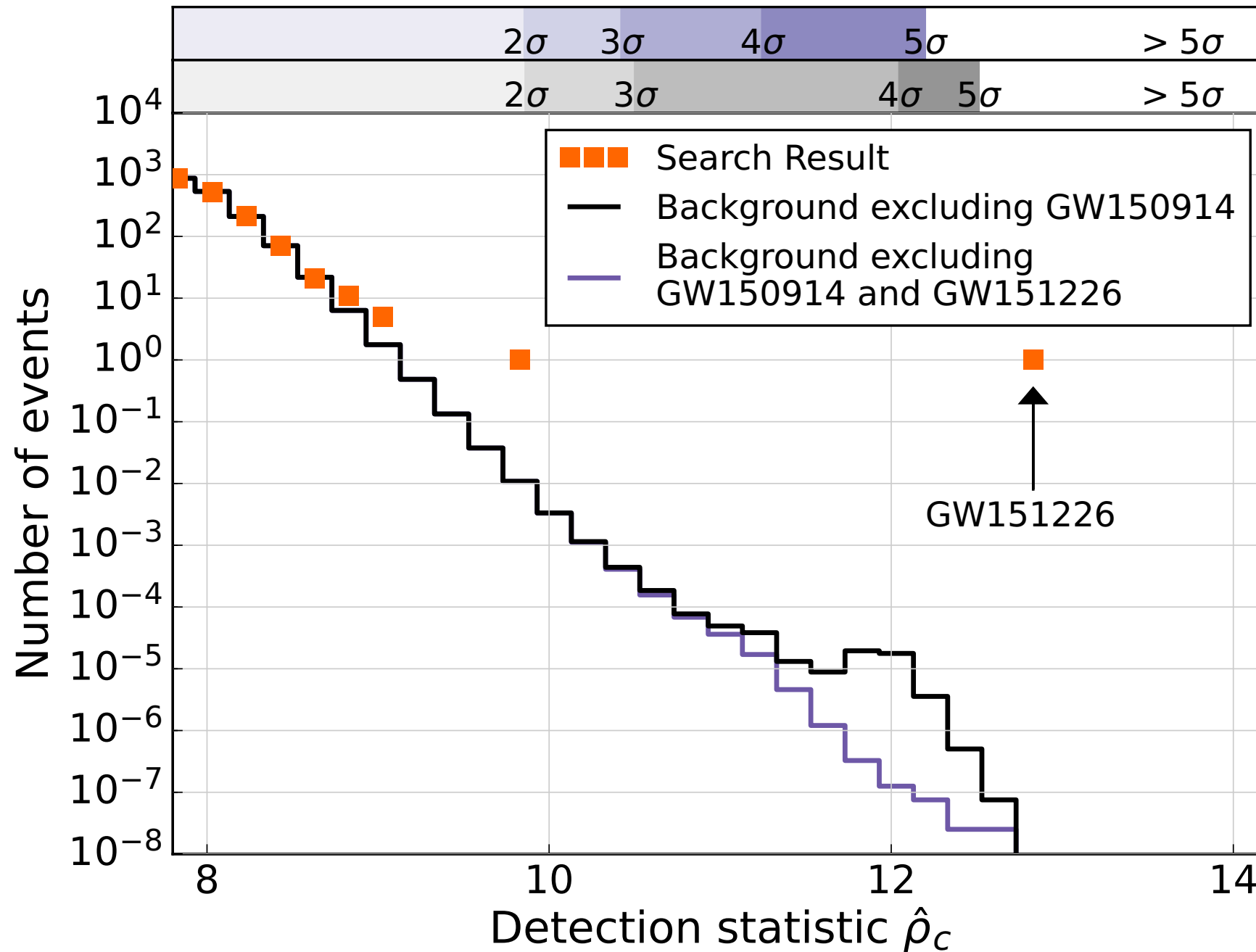
Detection confidence with modeled search in O1

(Abbott et al. arXiv:1606.04856)



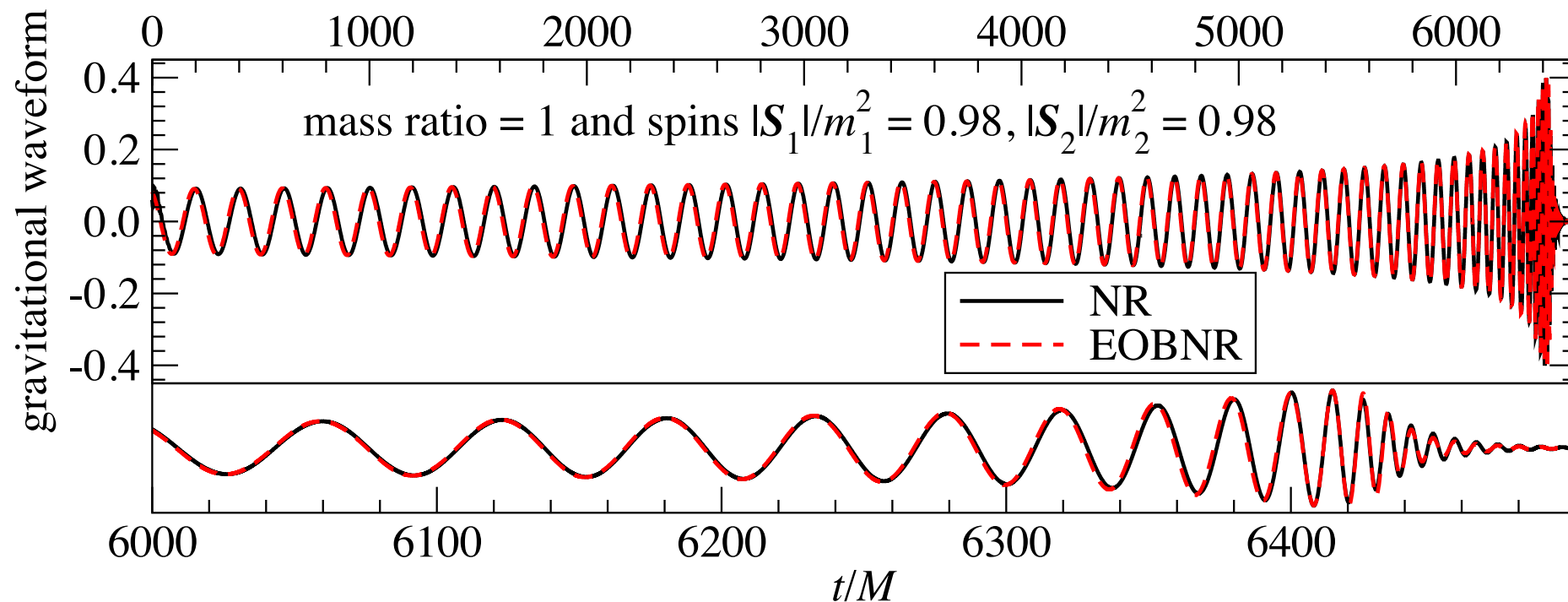
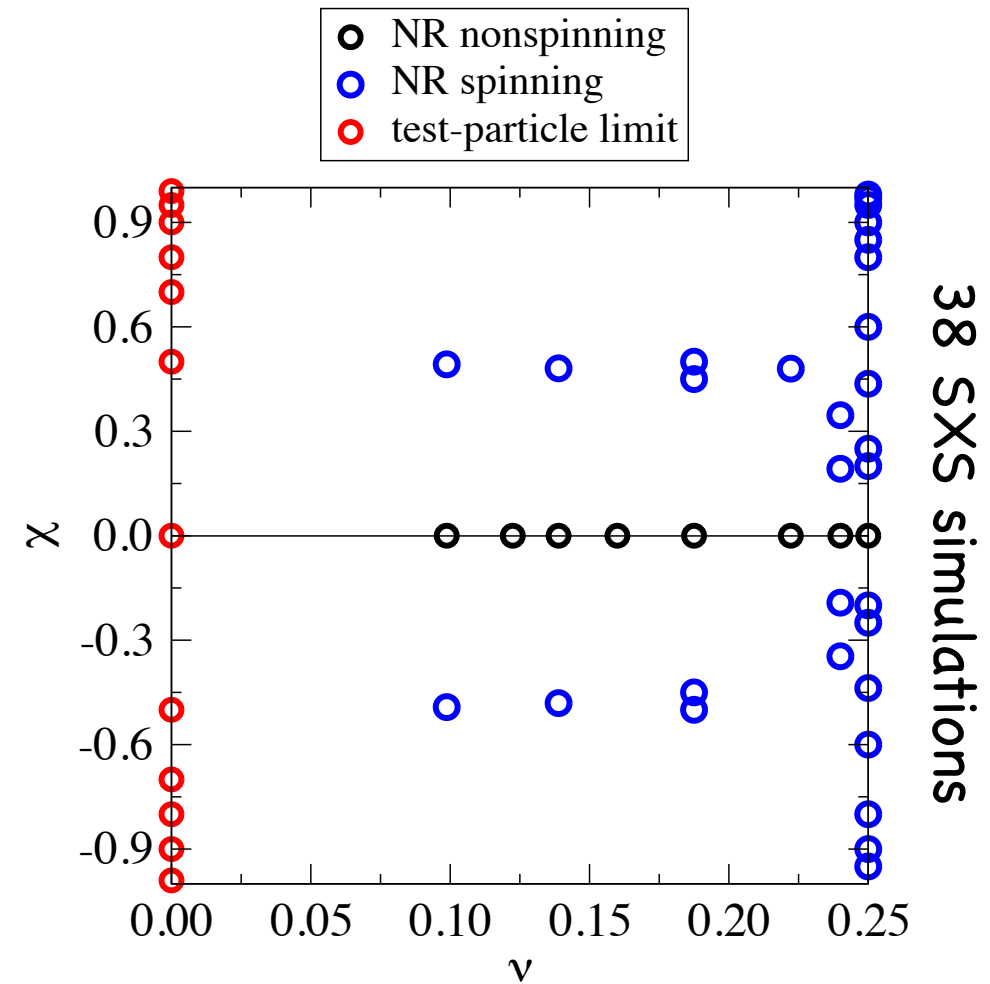
Detection confidence with modeled search in O1

(Abbott et al. arXiv:1606.04856)



EOBNR waveforms used in LIGO O1

- EOB waveforms with **nonprecessing spins** calibrated to NR waveforms (Taracchini, AB, Pan, Hinderer & SXS 14)
(Barausse & AB 10, 11, Barausse et al. 09, Damour & Nagar 09, Pan et al. 08, Damour et al. 08)

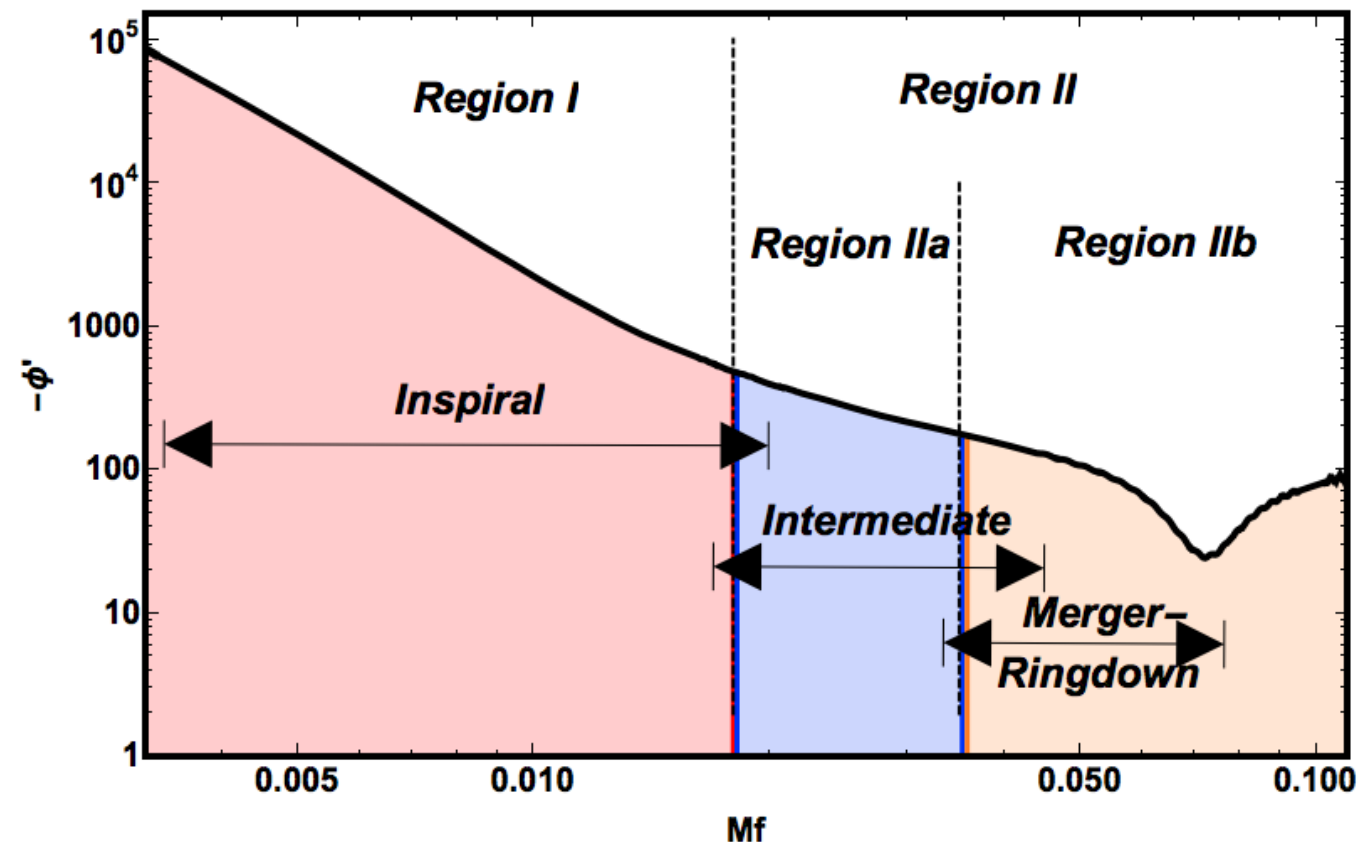
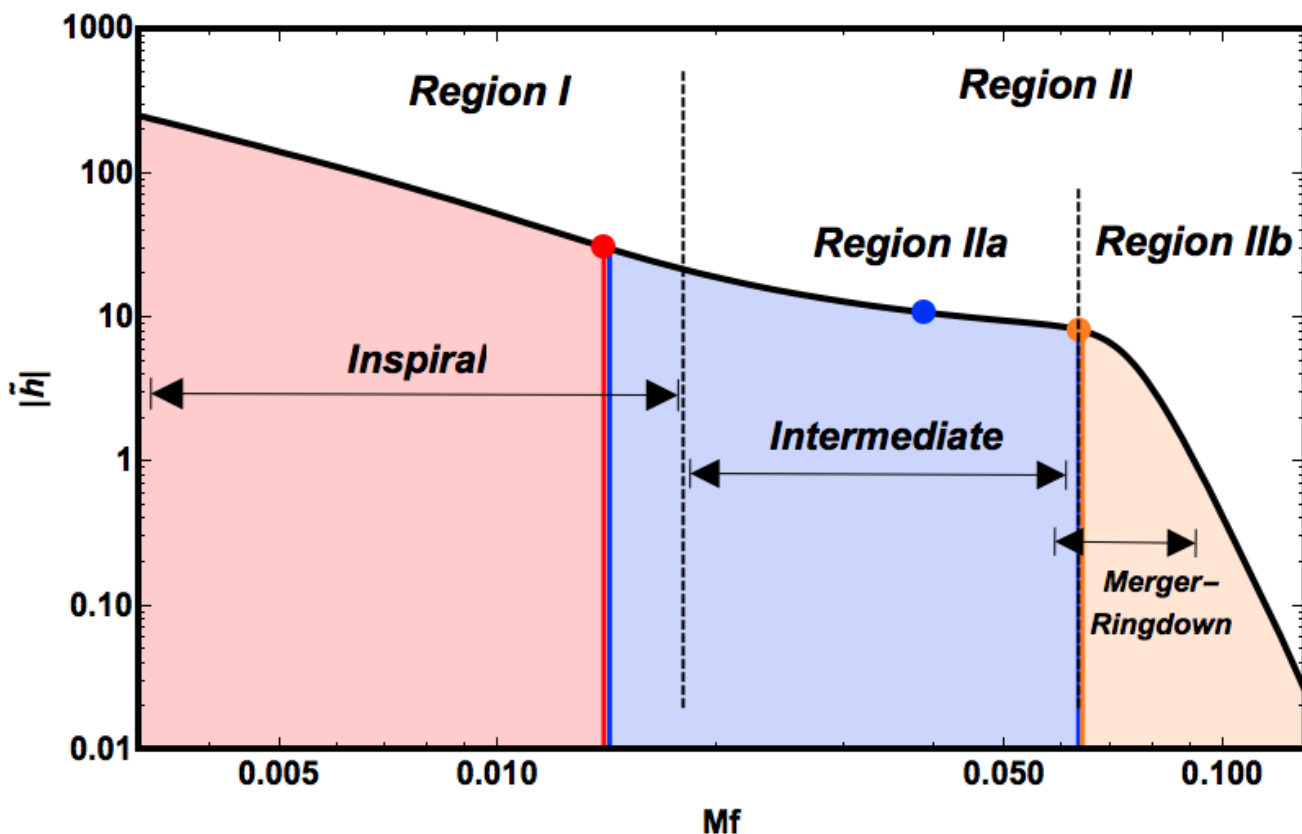


(Taracchini et al. 14)

IMR phenomenological waveforms used in LIGO O1

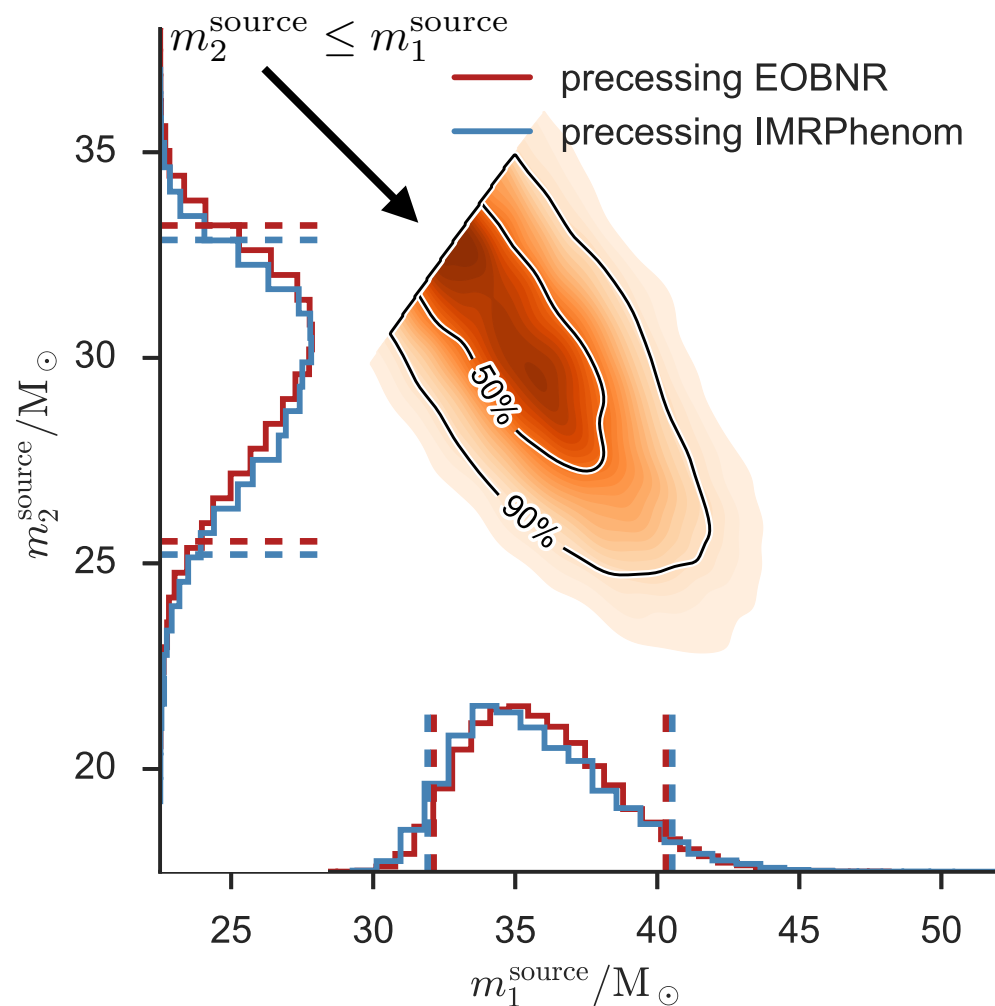
- First works in mid-late 2000 (Ajith et al. 07, Pan et al. 07, Ajith et al. 11, Santamaria et al. 10)
- **Fast, frequency-domain** waveform model hybridizing and fitting EOB & NR (Khan et al. 15; Husa et al. 15)

$$\tilde{h}(f; \lambda_i) = \mathcal{A}(f; \lambda_i) e^{i\phi(f; \lambda_i)}$$

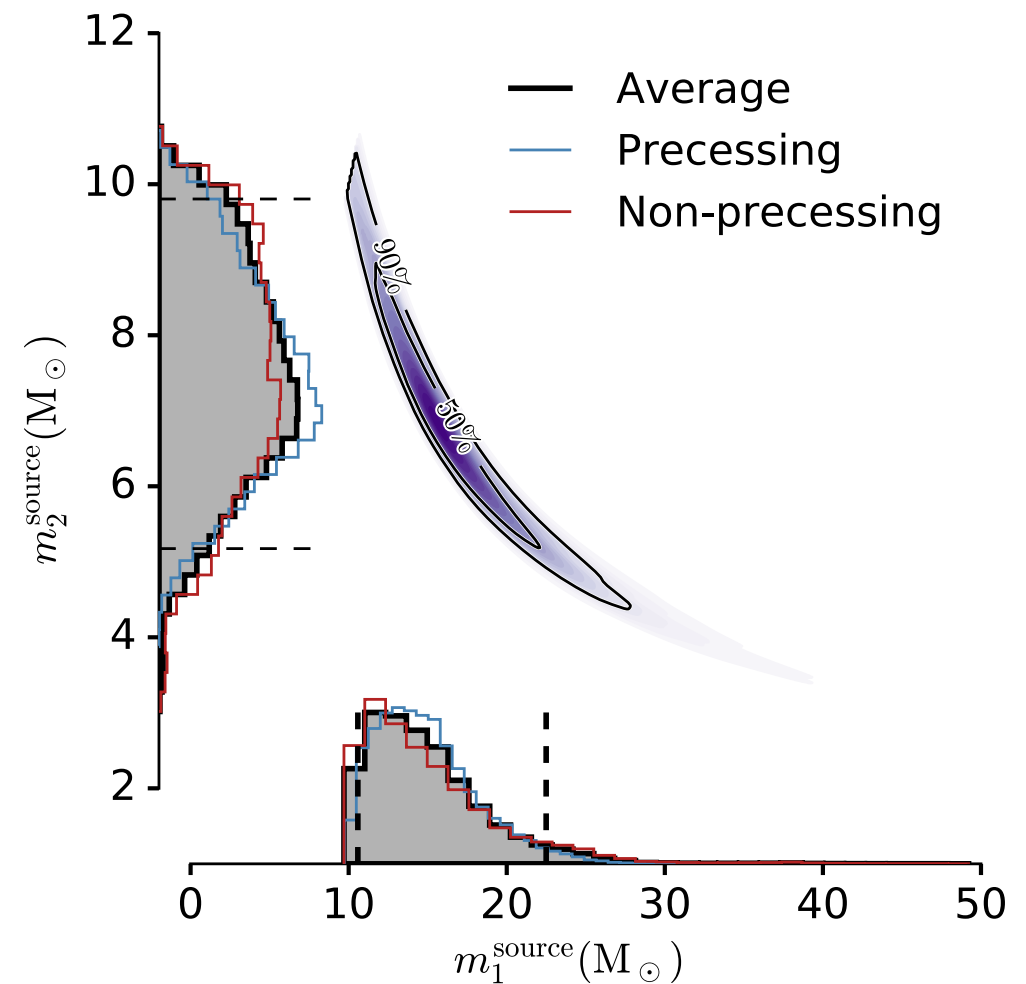


Unveiling binary black holes properties: masses

GW150914



GW151226



(Abbott et al. PRX 6 (2016) 041014)

(Abbott et al. PRL 116 (2016) 241103)

- We **measure best** the “**chirp**” mass $\mathcal{M} = M \nu^{3/5}$
- **GW150914**: merger in band, total mass well measured, good measurement of individual masses.
- **GW151226**: merger outside band, individual masses measured less precisely.

Effect of total mass on the waveform

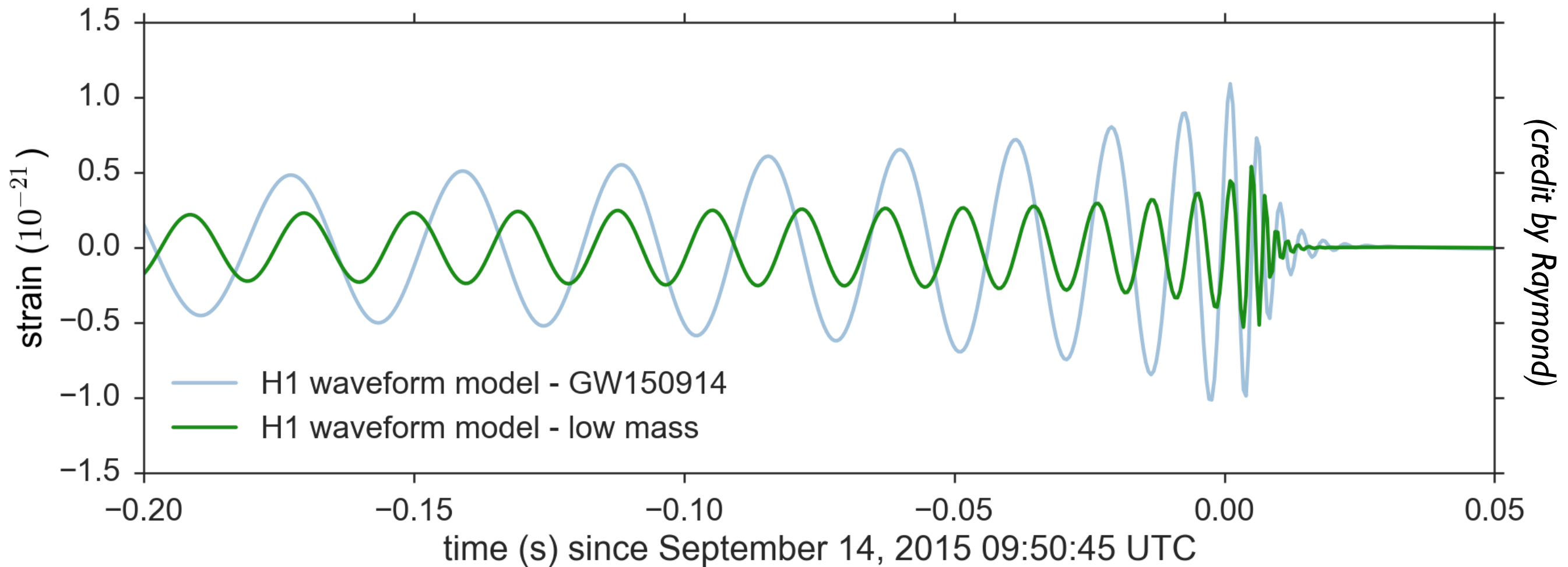
$$\mathcal{M} = 30.4M_{\odot} \quad q = 1.24$$



$$\mathcal{M} = 15.2M_{\odot} \quad q = 1.24$$

$$\mathcal{M} = M \nu^{3/5}$$

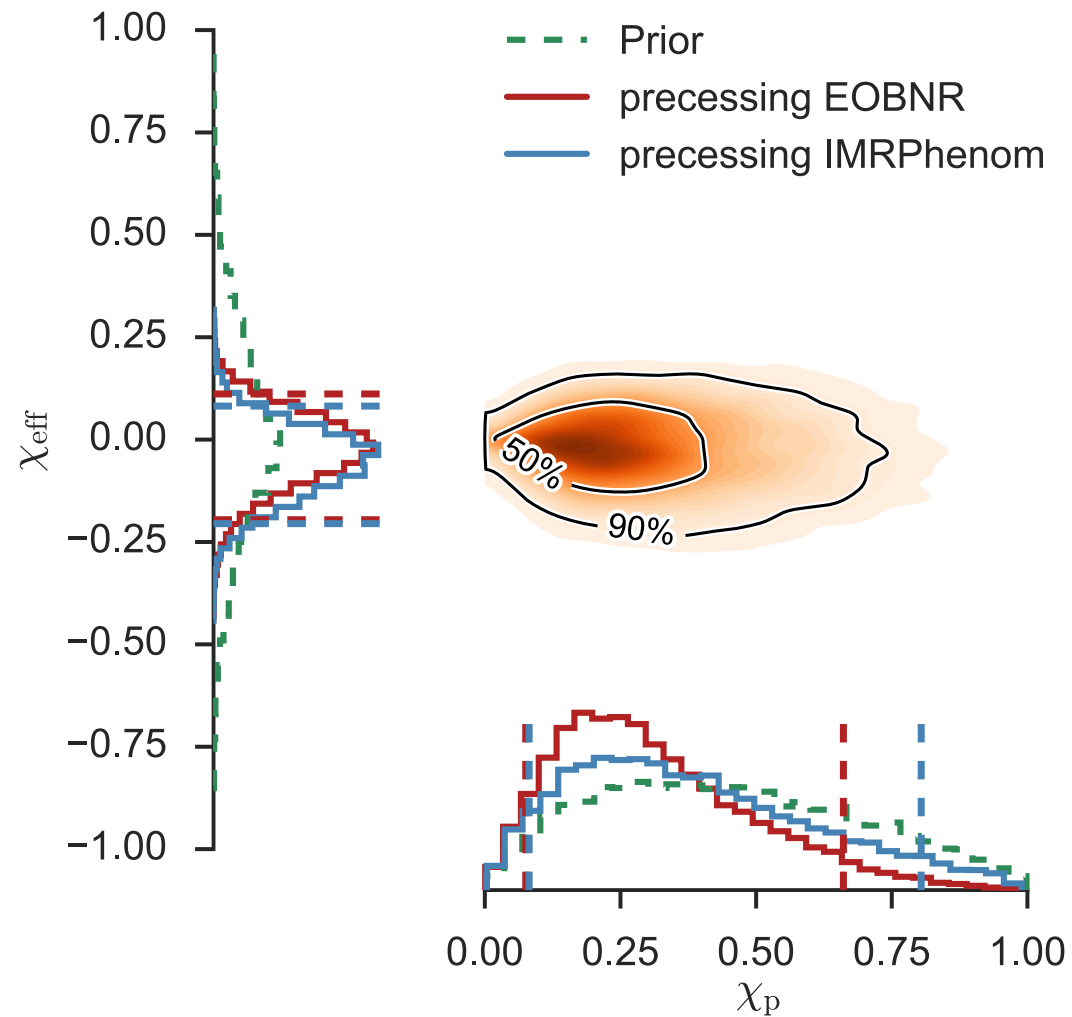
$$\nu = \frac{q}{(1+q)^2}$$



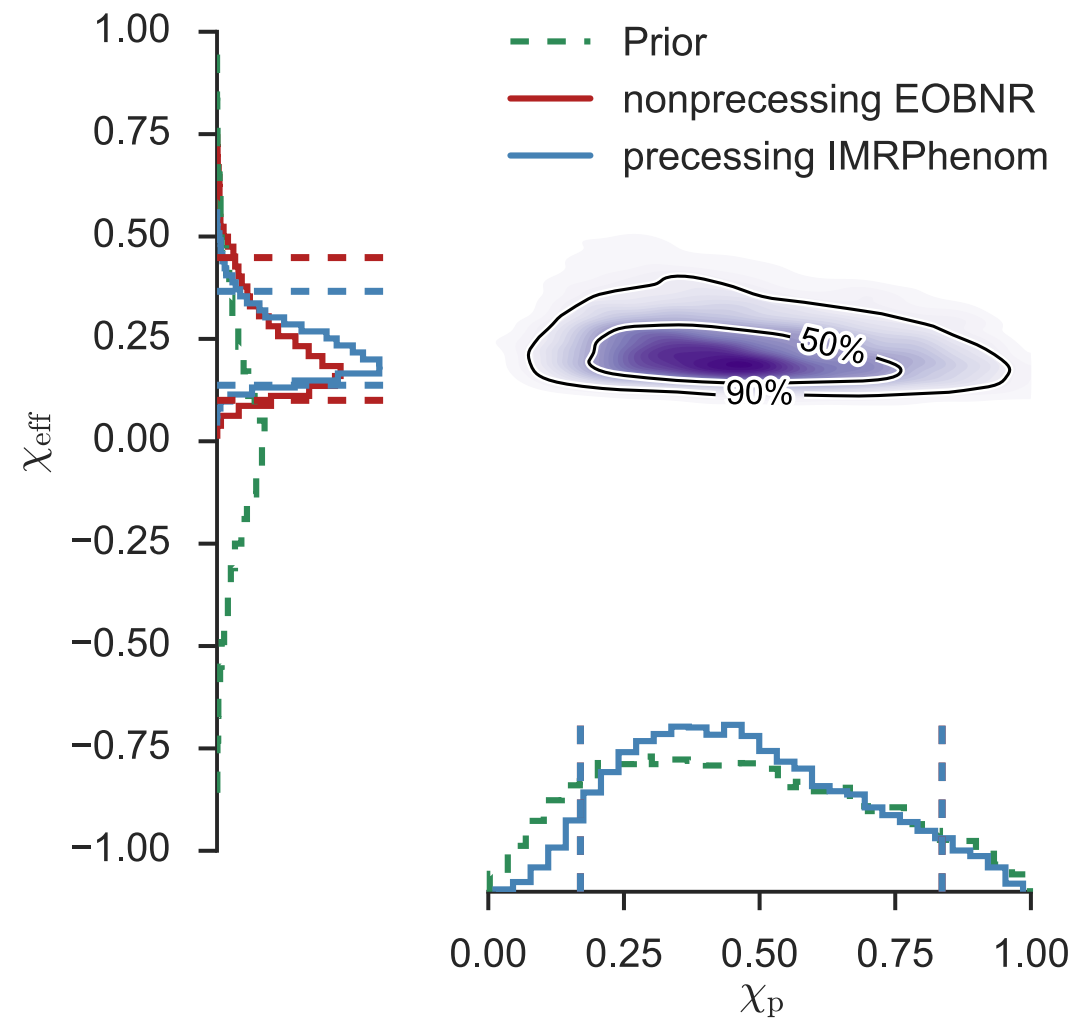
Unveiling binary black-holes properties: spins

(Abbott et al. PRX 6 (2016) 041014)

GW150914



GW151226



(Abbott et al. PRL 116 (2016) 241103)

- BHs' spins not maximal, and for GW151226 one BH's spin larger than 0.2 at 99% confidence.

$$\chi_{\text{eff}} = \left(\frac{\mathbf{S}_1}{m_1} + \frac{\mathbf{S}_2}{m_2} \right) \cdot \left(\frac{\hat{\mathbf{L}}}{M} \right)$$

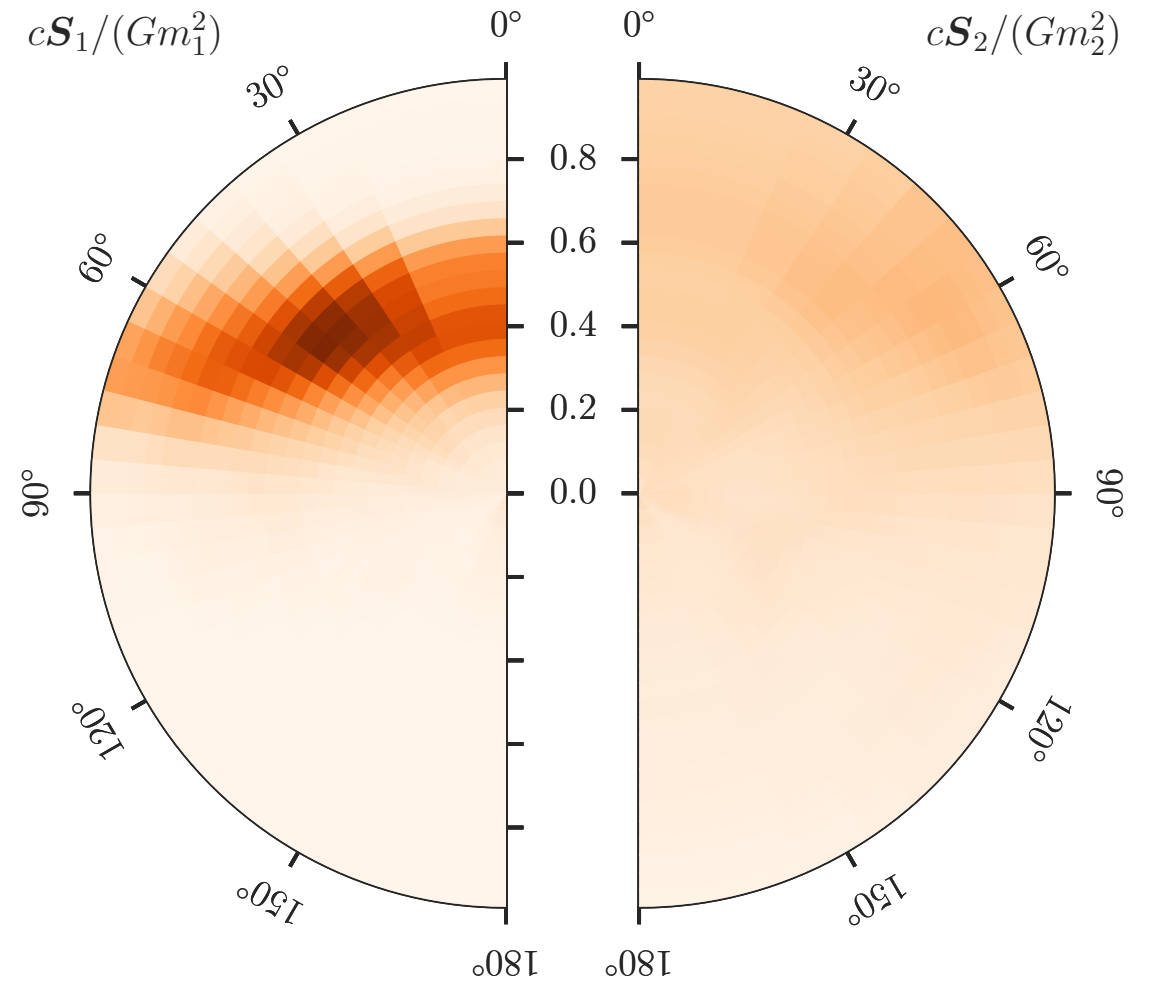
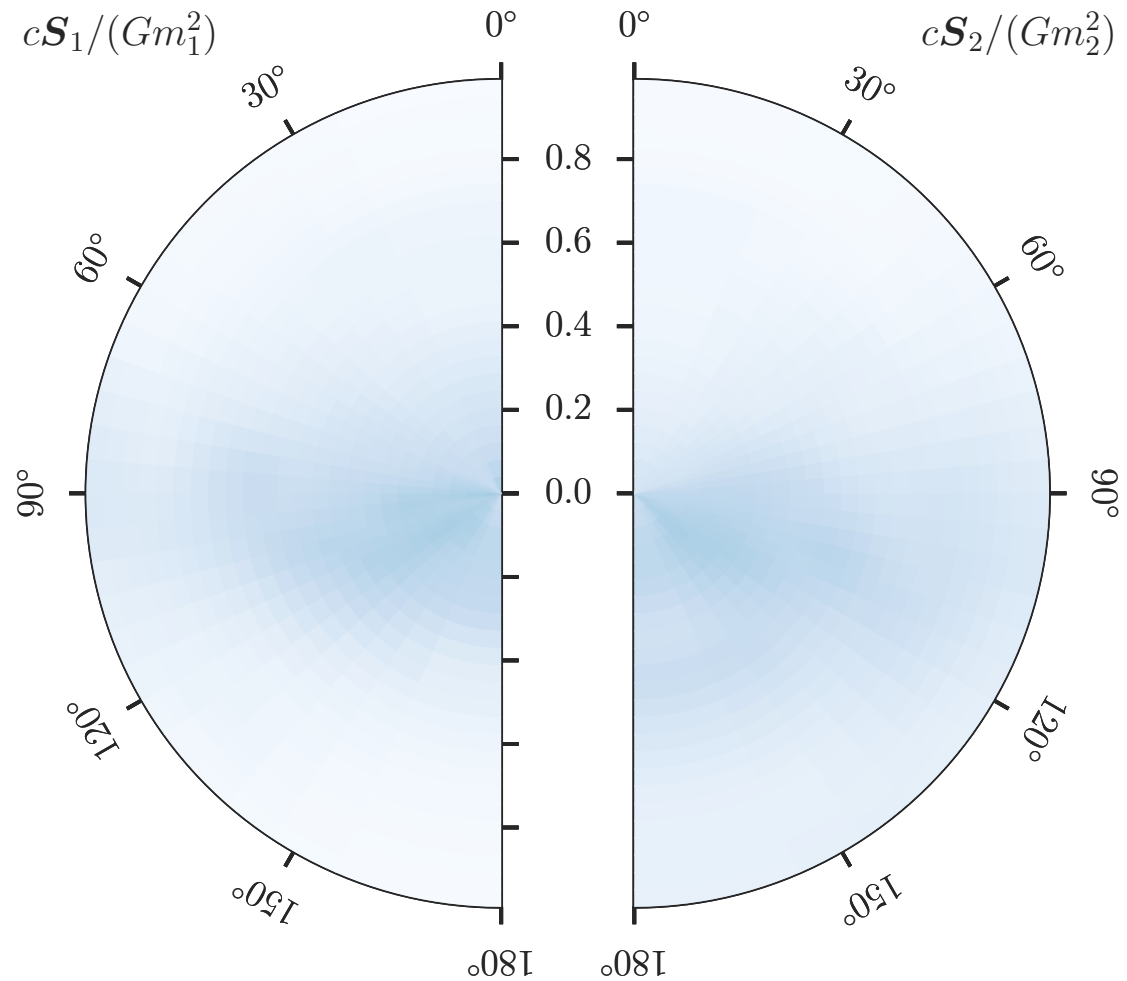
- Spin of primary BH < 0.7. No information about precession.

Unveiling binary black-holes properties: spins

GW150914

GW151226

(Abbott et al. arXiv:1606.01210)

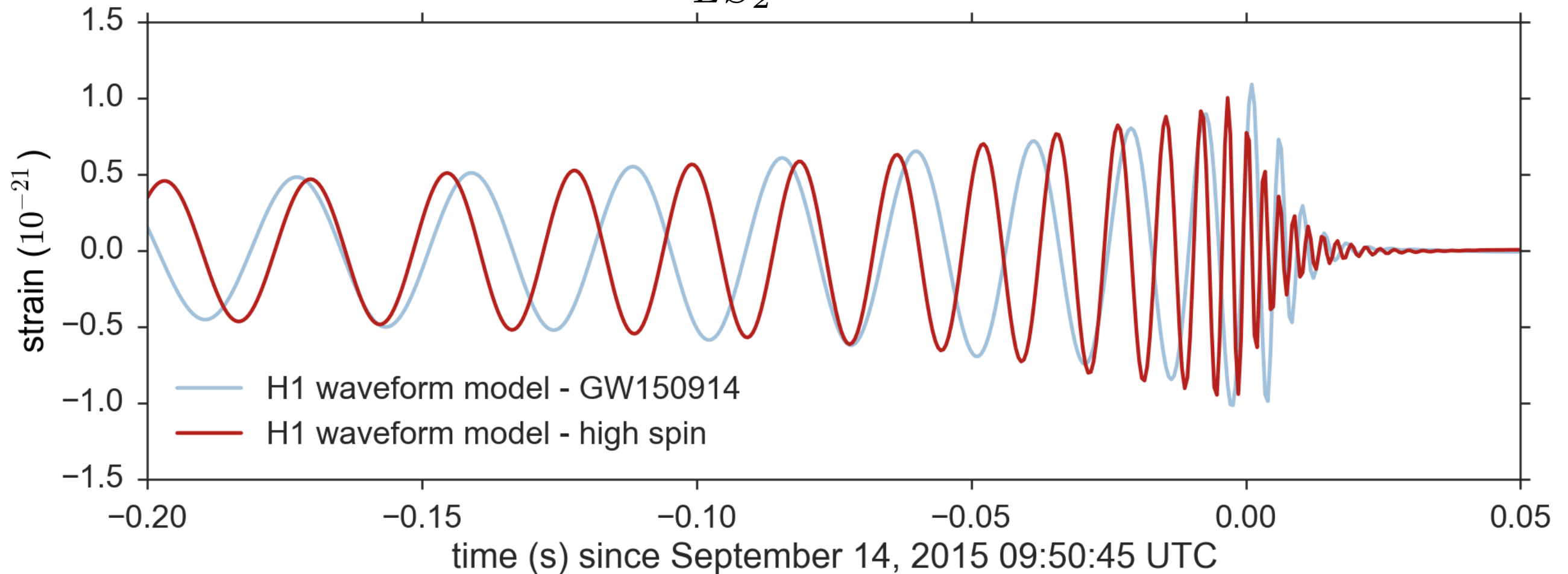
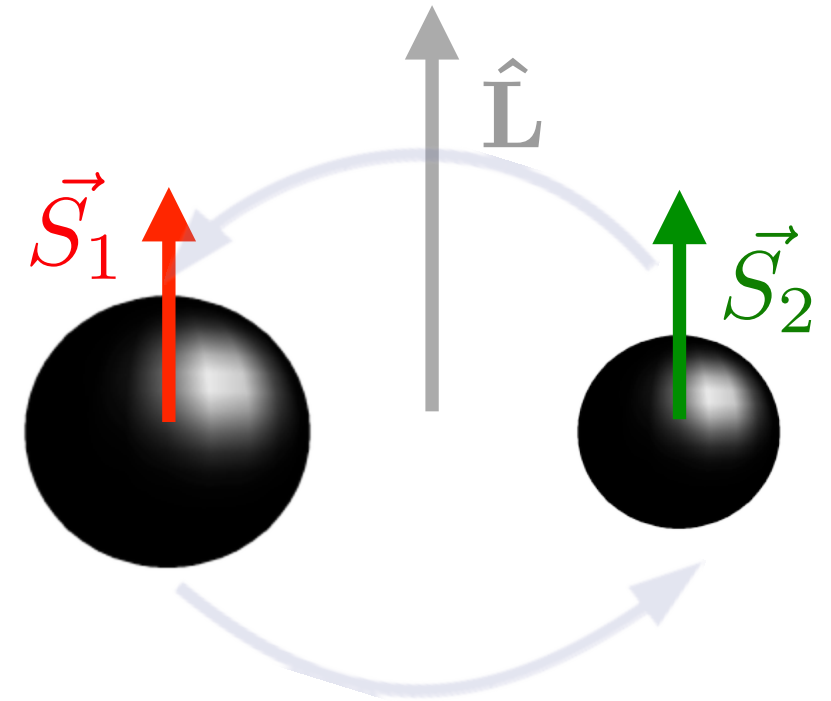


- Bins are constructed linearly in spin magnitude & cosine of tilt angles

$$\cos \theta_{LS_i} = \hat{\mathbf{S}}_i \cdot \hat{\mathbf{L}}$$

Effect of aligned spins on the waveform

$\mathcal{M} = 30.4M_{\odot}$	$\mathcal{M} = 30.4M_{\odot}$
$q = 1.24$	$q = 1.24$
$\chi_1 = 0.81$	$\chi_1 = 0.99$
$\chi_2 = 0.54$	$\chi_2 = 0.99$
$\theta_{LS_1} = 116^{\circ}$	$\theta_{LS_1} = 0^{\circ}$
$\theta_{LS_2} = 15^{\circ}$	$\theta_{LS_2} = 0^{\circ}$



(credit by Raymond)

Effect of precessing spins/mass ratio on the waveform

$$\mathcal{M} = 30.4M_{\odot}$$

$$q = 1.24$$

$$\chi_1 = 0.81$$

$$\chi_2 = 0.54$$

$$\theta_{LS_1} = 116^{\circ}$$

$$\theta_{LS_2} = 15^{\circ}$$

$$\mathcal{M} = 30.4M_{\odot}$$

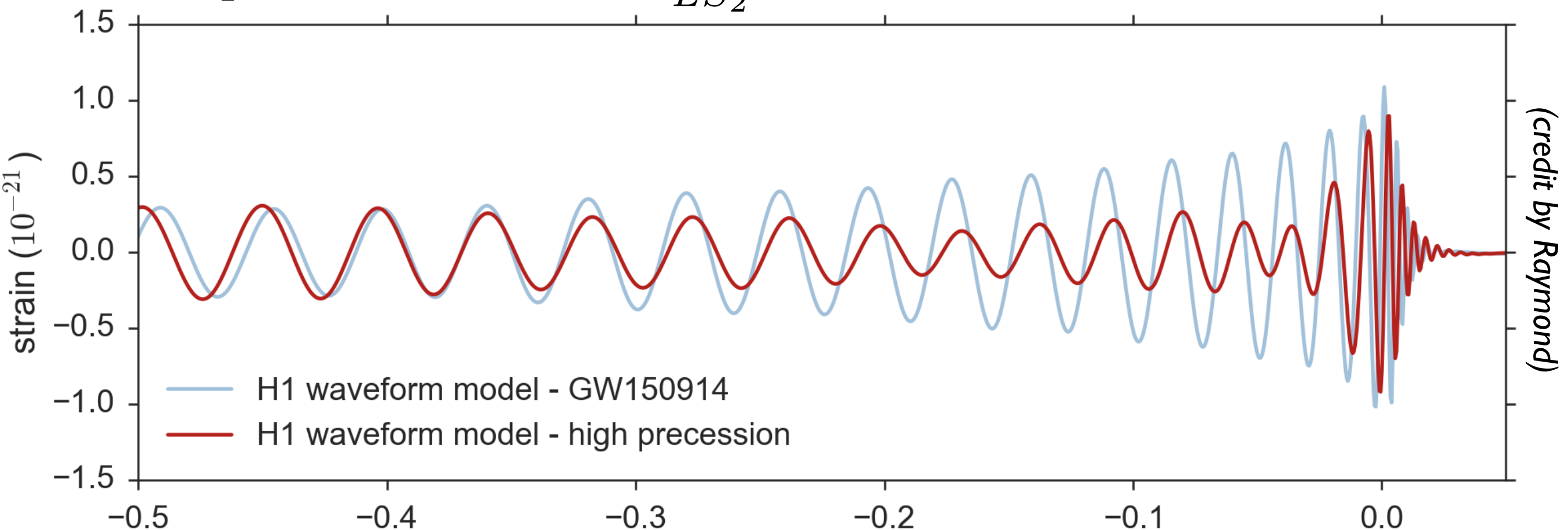
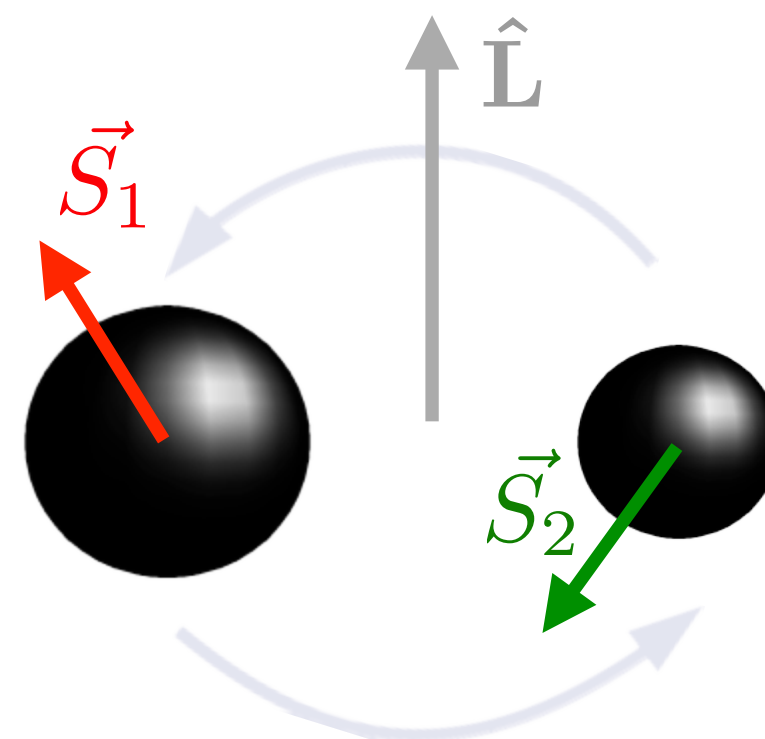
$$q = 4$$

$$\chi_1 = 0.99$$

$$\chi_2 = 0.99$$

$$\theta_{LS_1} = 45^{\circ}$$

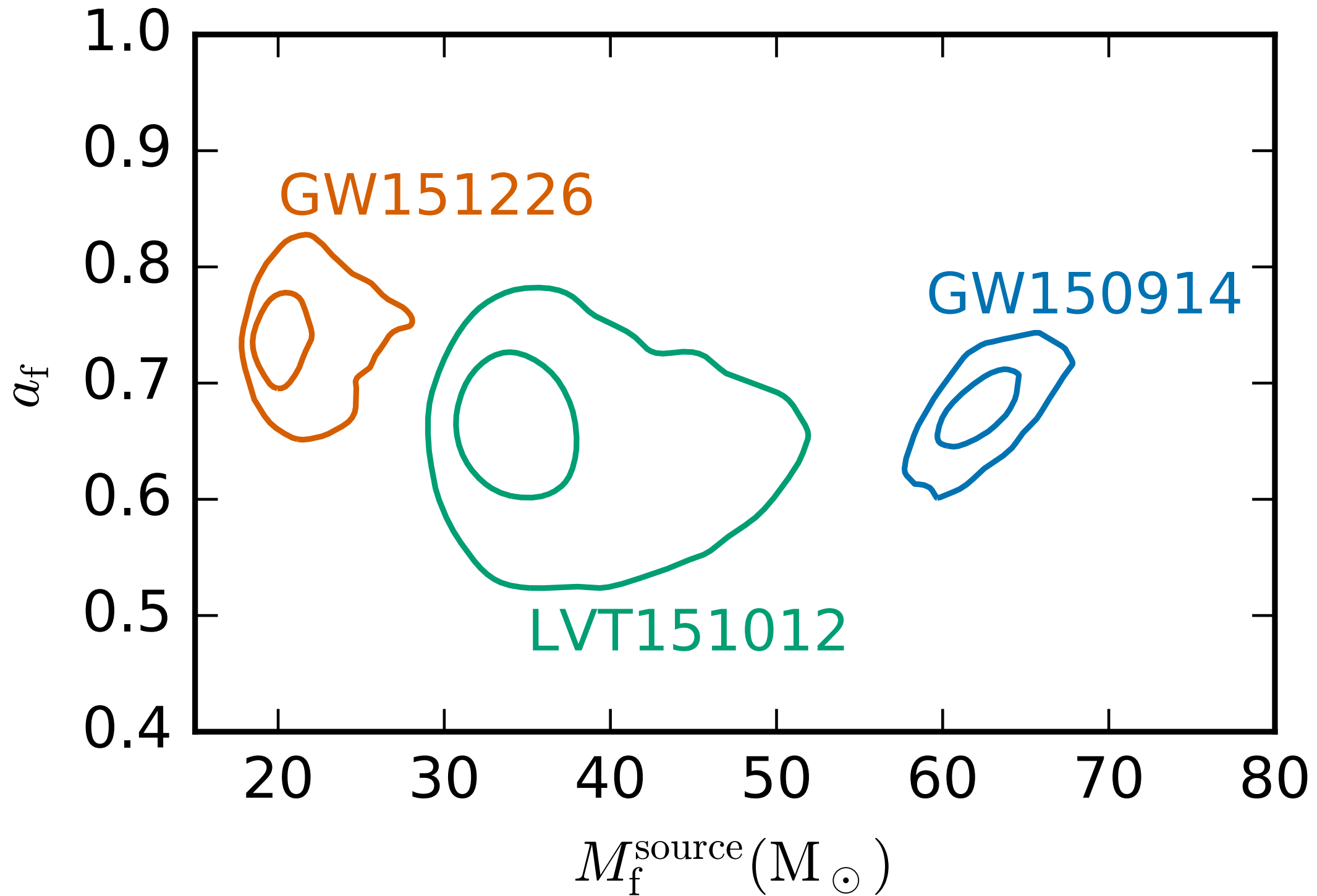
$$\theta_{LS_2} = 30^{\circ}$$



Properties of final black hole formed after merger

(Abbott et al. arXiv:1606.04856)

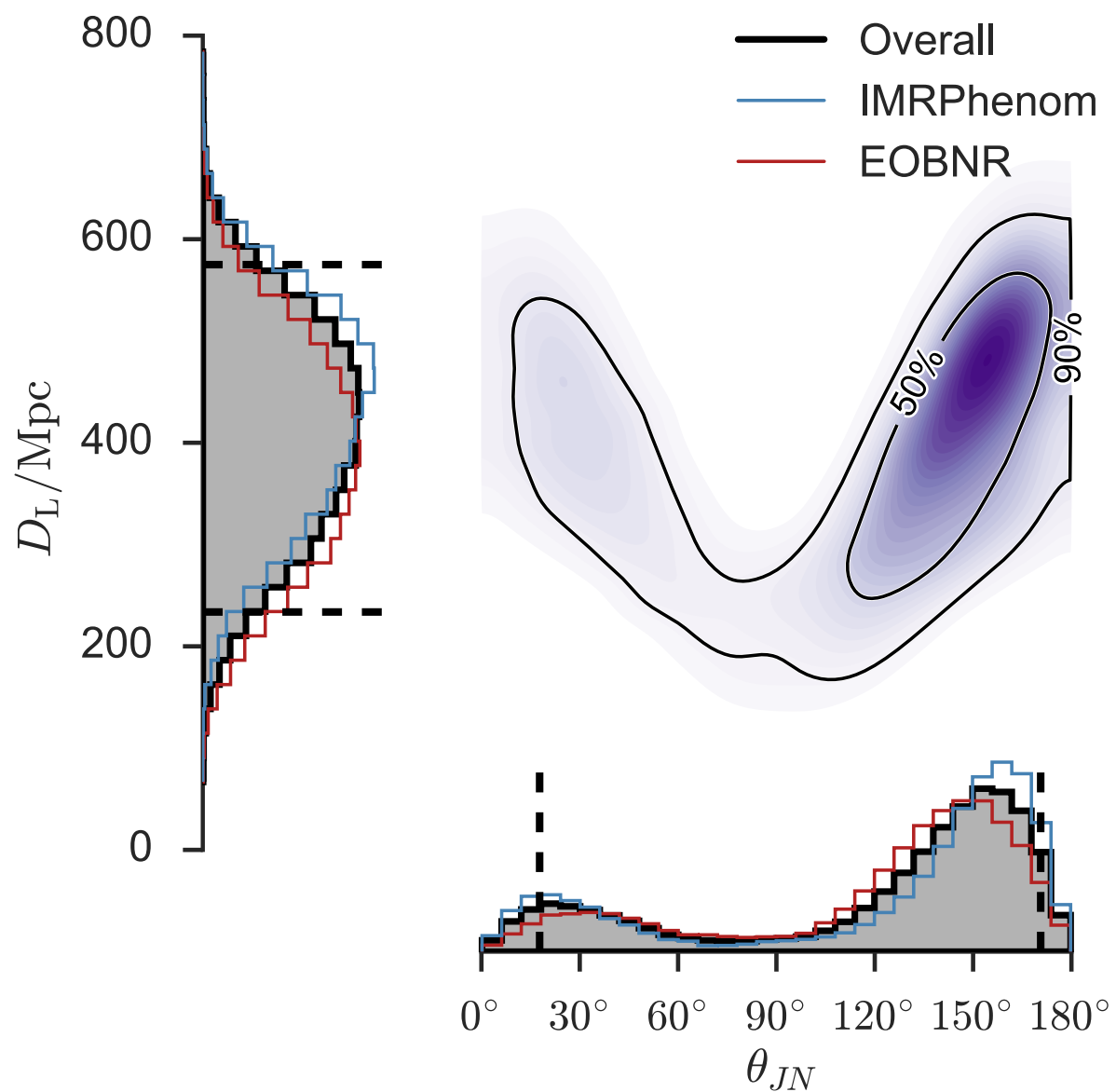
(Abbott et al. arXiv:1606.01210)



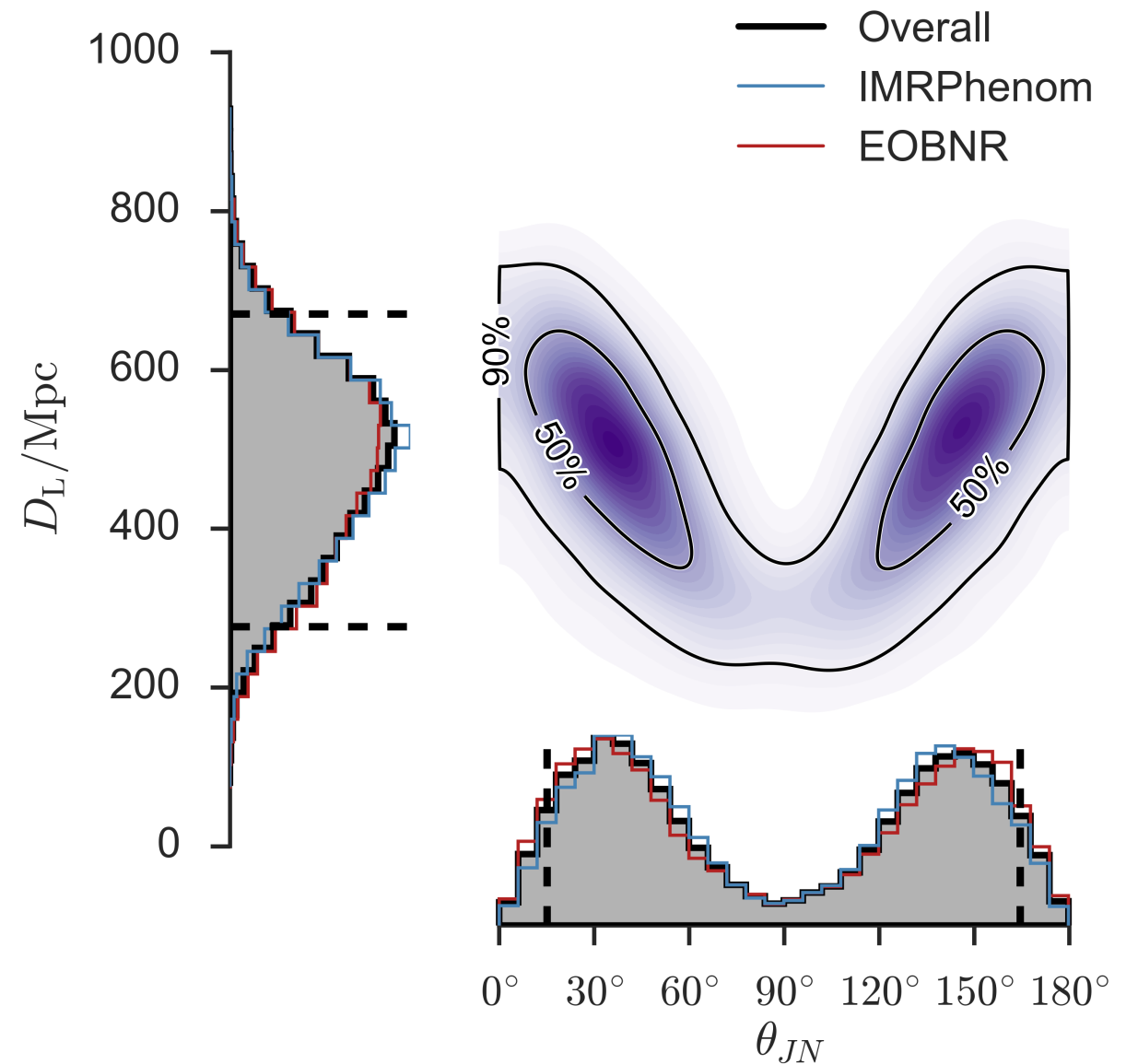
Binaries' distance and orbital-plane inclination with respect to line of sight

(Abbott et al. arXiv:1606.04856)

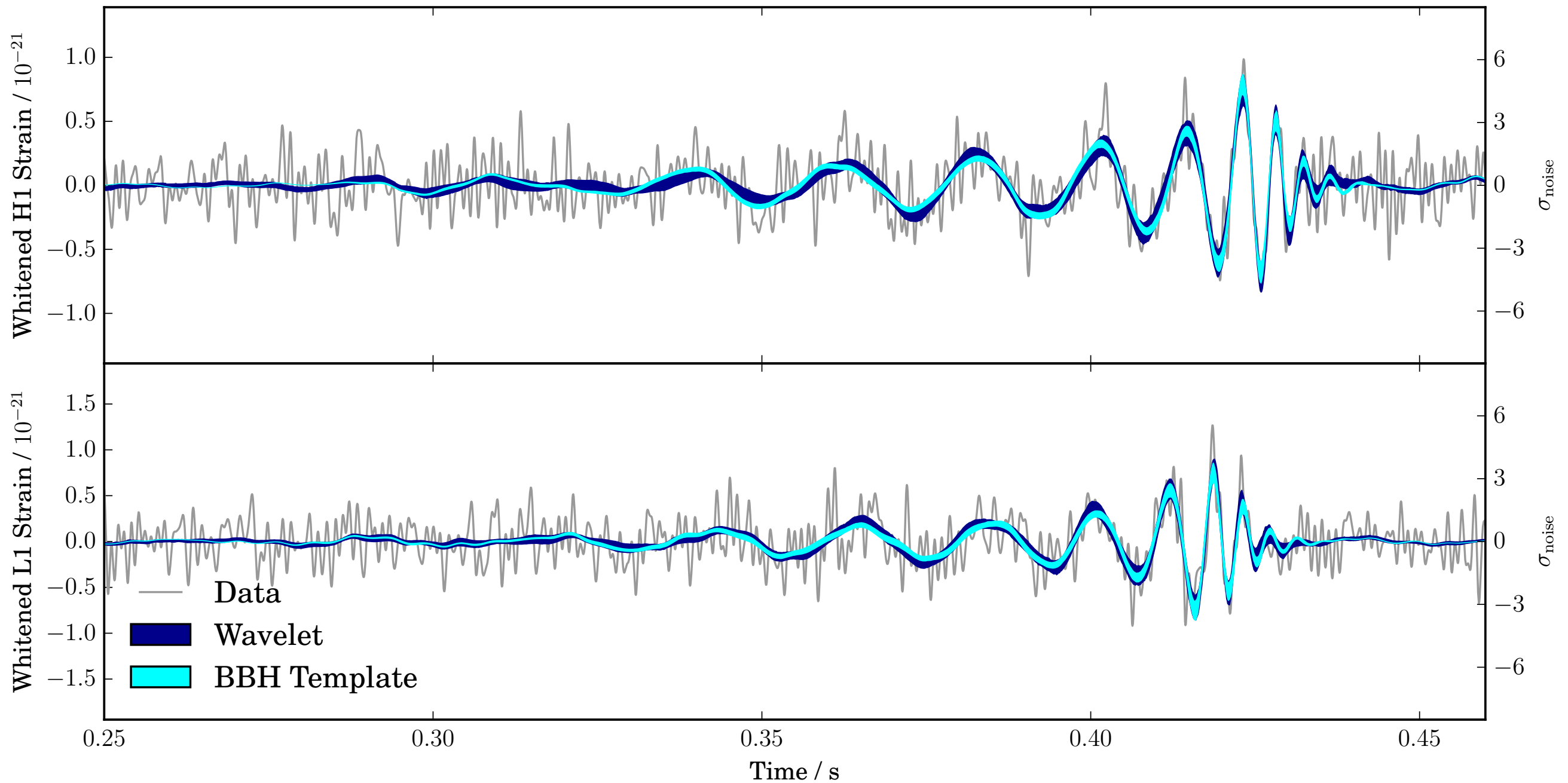
GW150914



GW151226

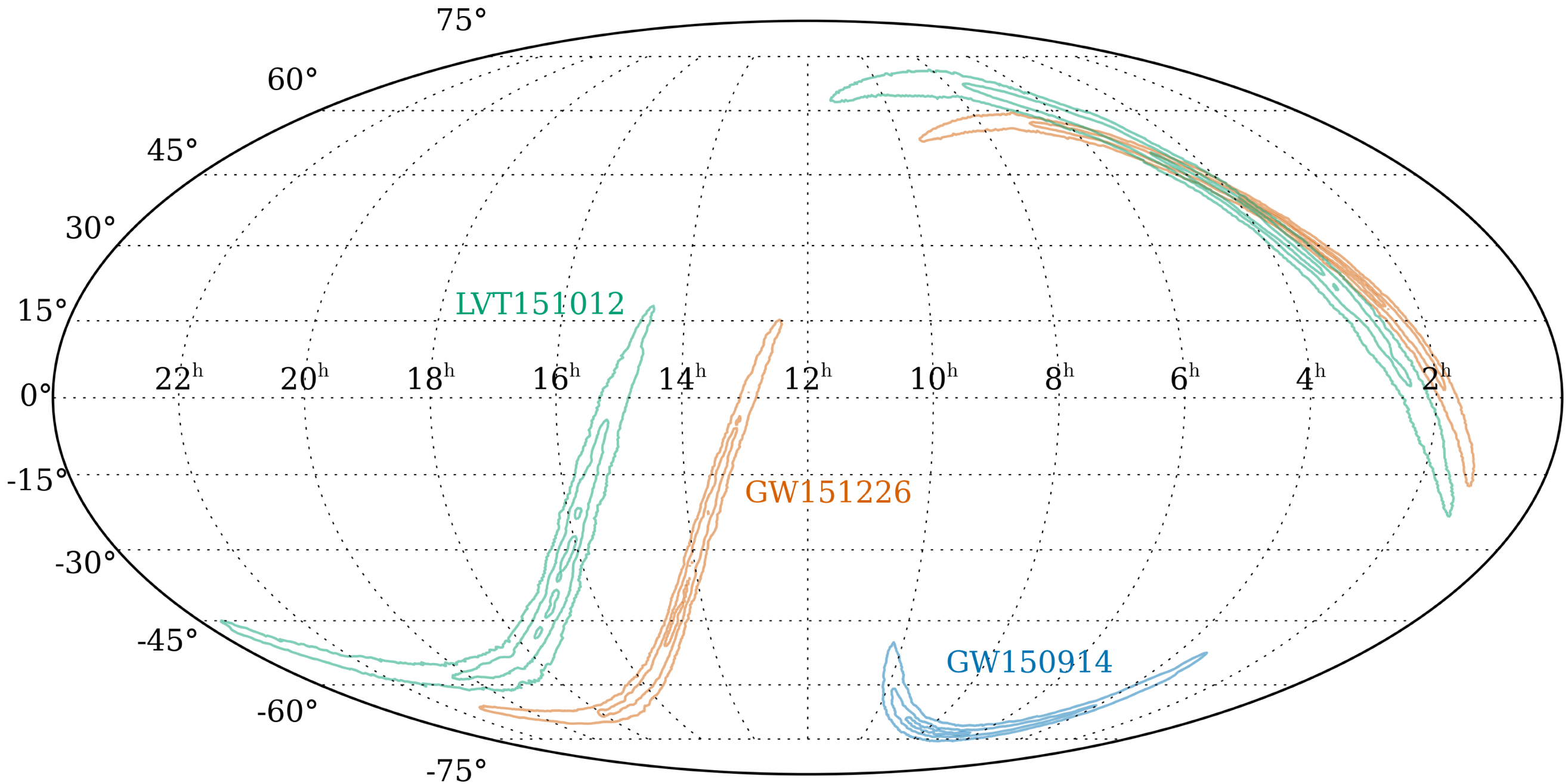


Time-domain data and reconstructed waveforms

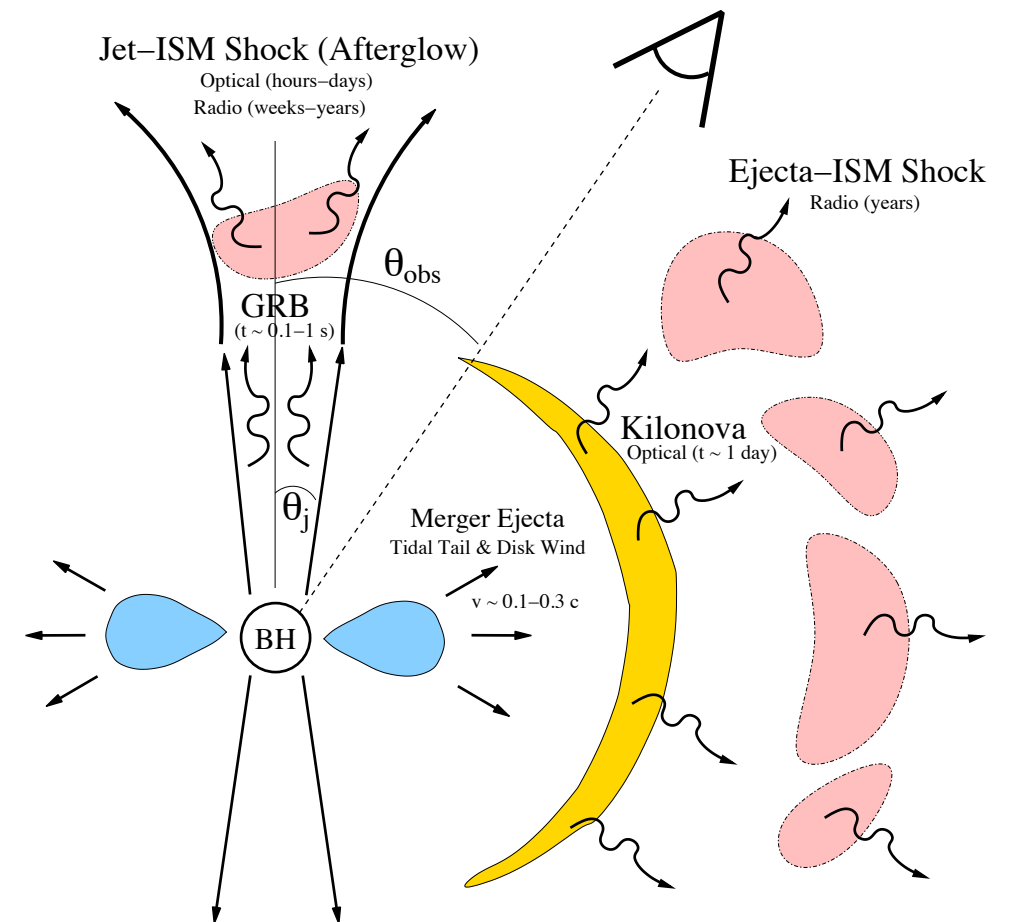
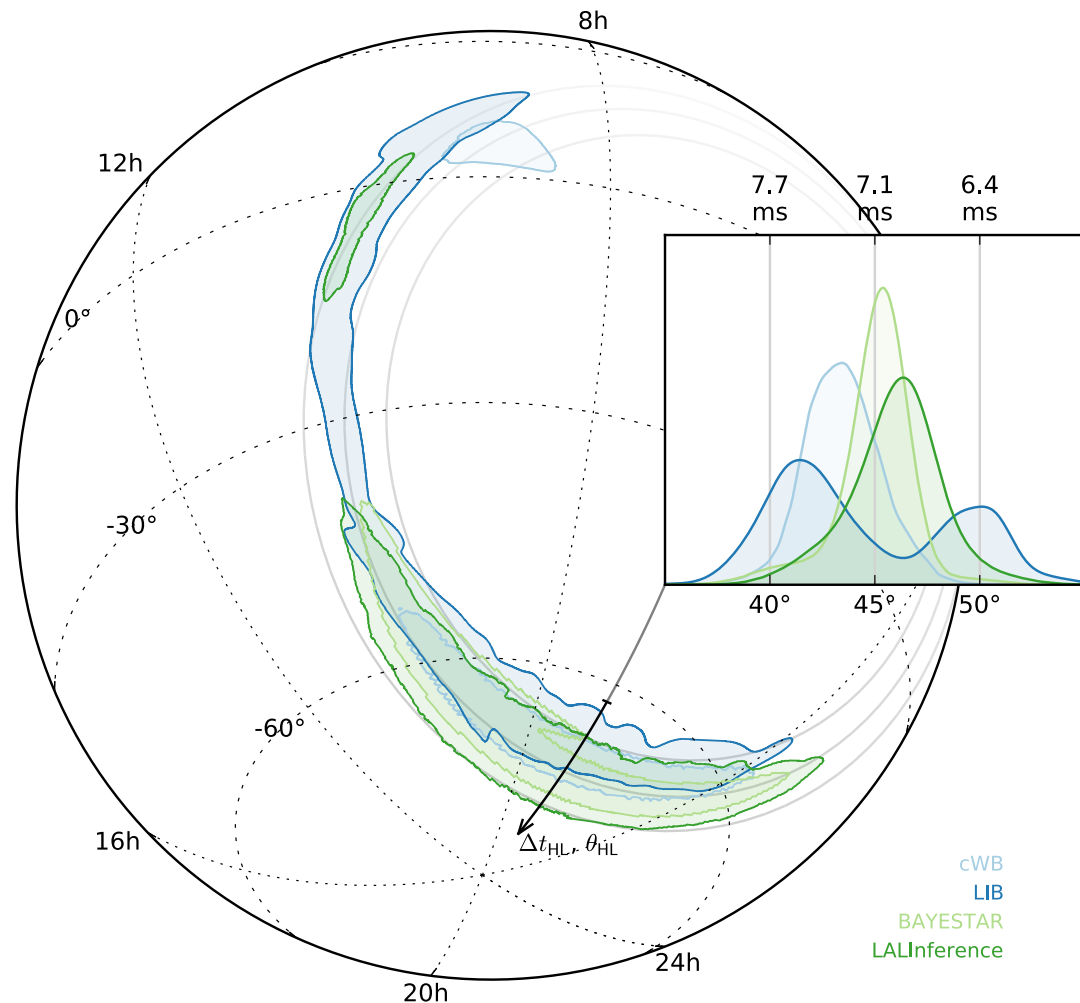
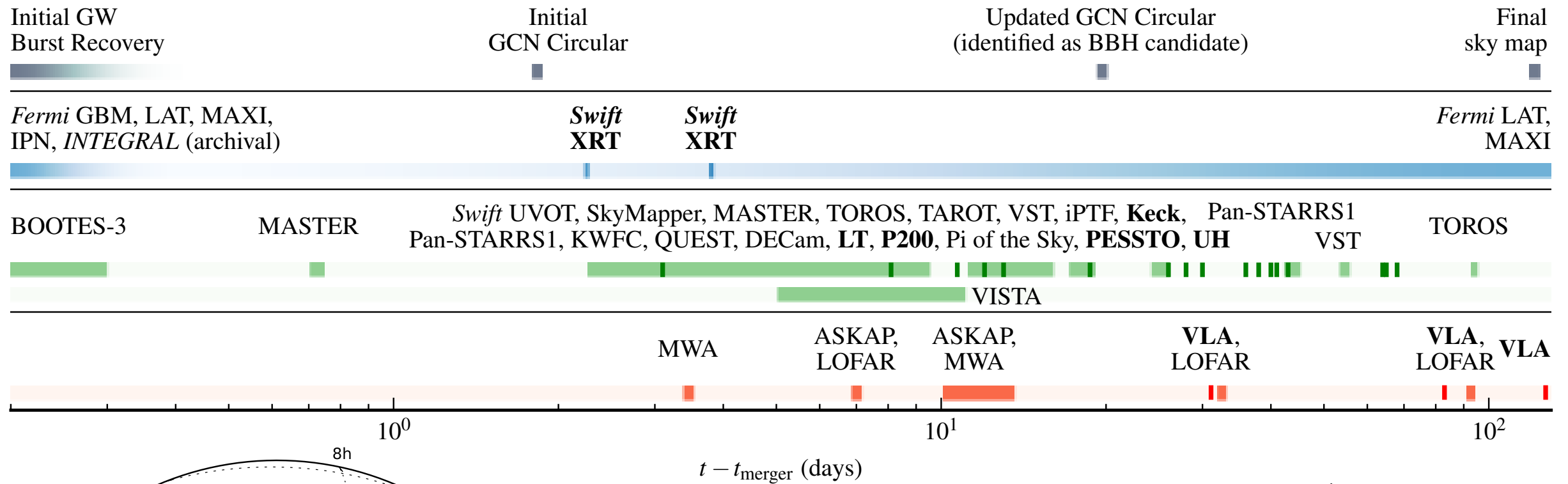


Sky map for all LIGO O1 events

(Abbott et al. arXiv:1606.04856)



First campaign for electromagnetic counterparts

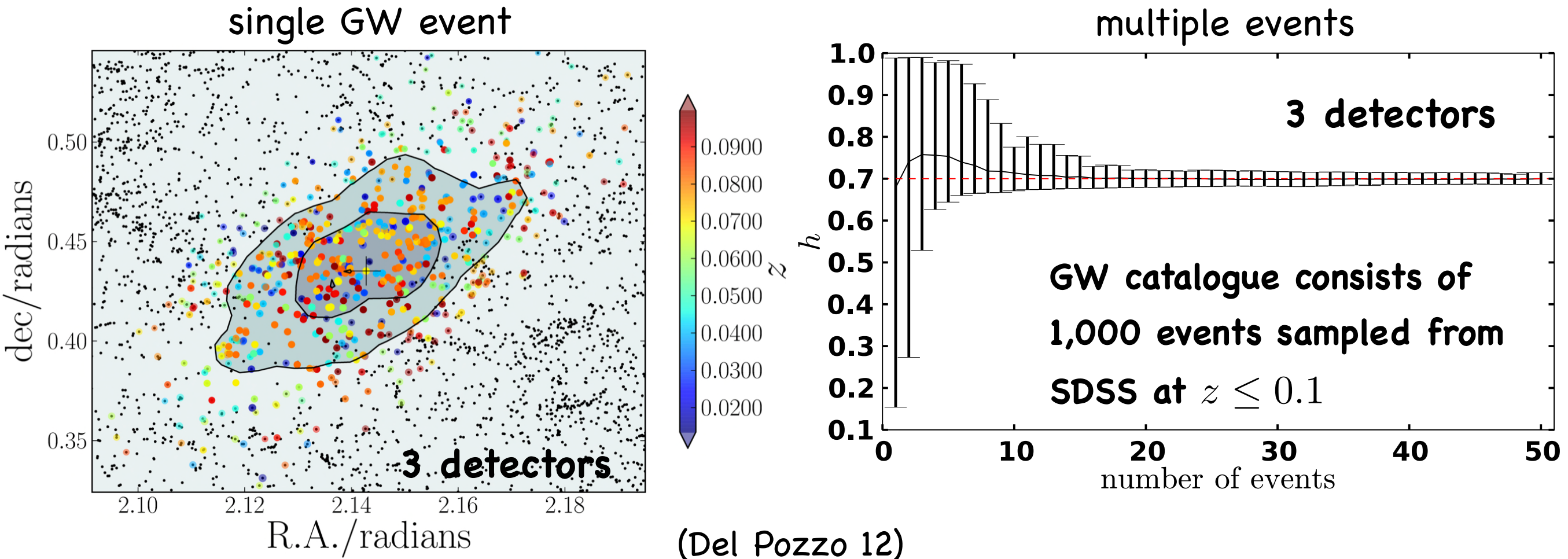


(Berger & Metzger 11)

Inference of cosmological parameters in future LIGO searches

- **Wide-field galaxy surveys** can provide (**sky positions** and) **redshifts**

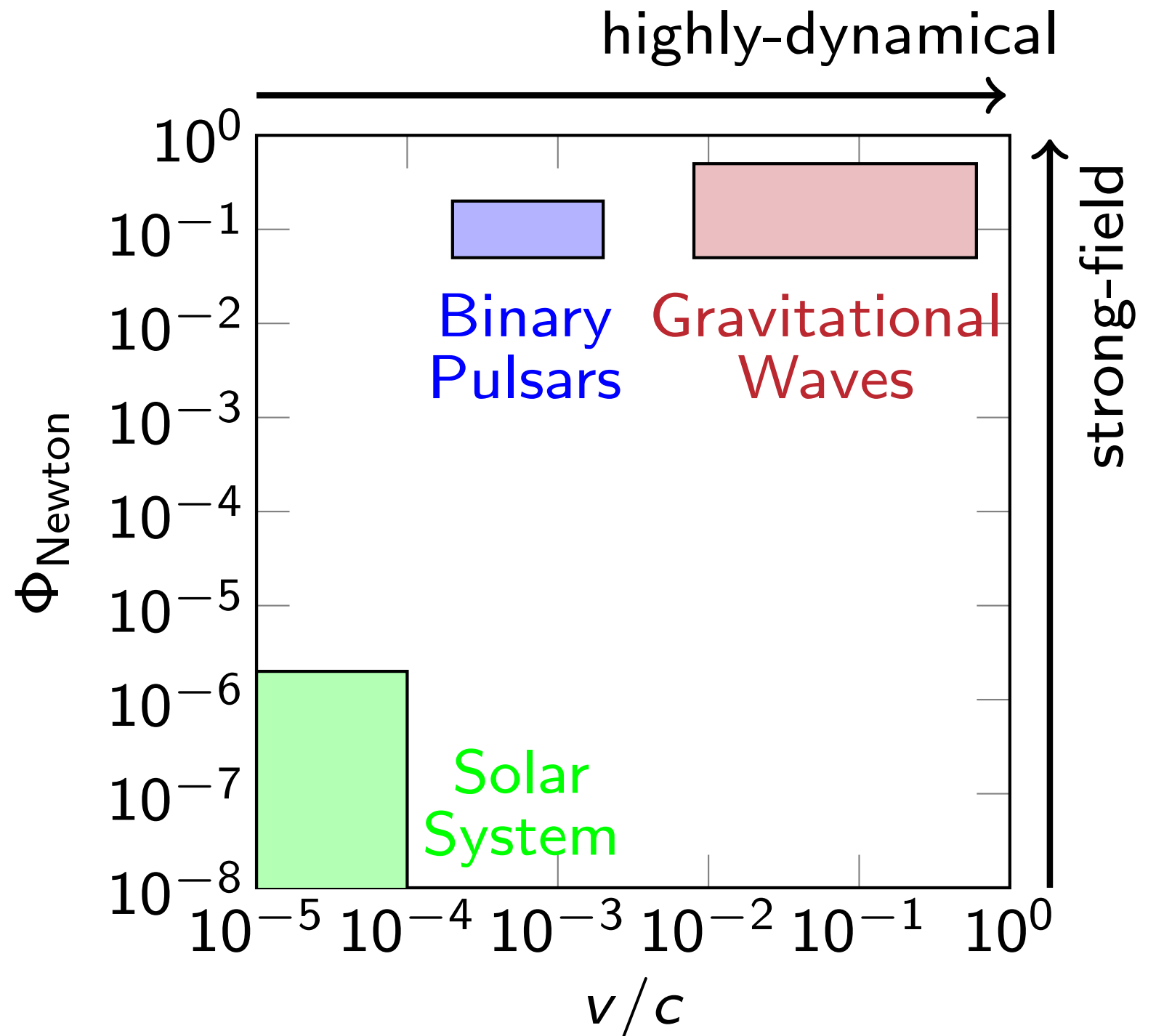
(Schutz 1986)



- Measurement of **Hubble constant** H_0 with accuracy of **5%** at 95% confidence **after 40-50 GW observations with 3 detectors.**

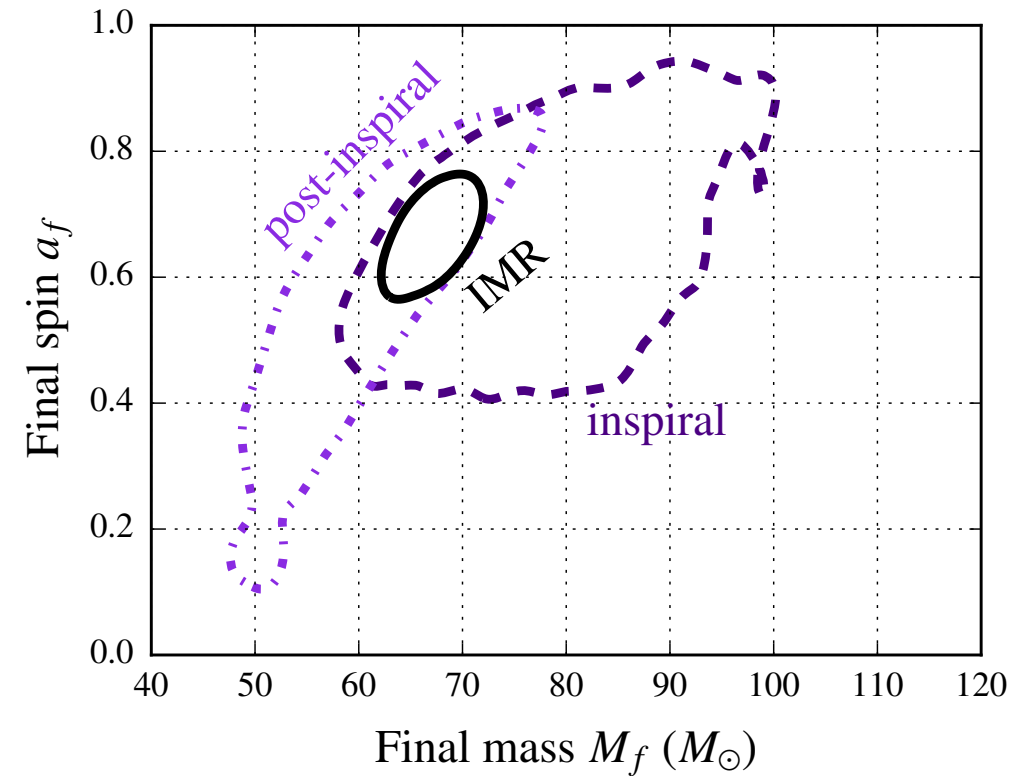
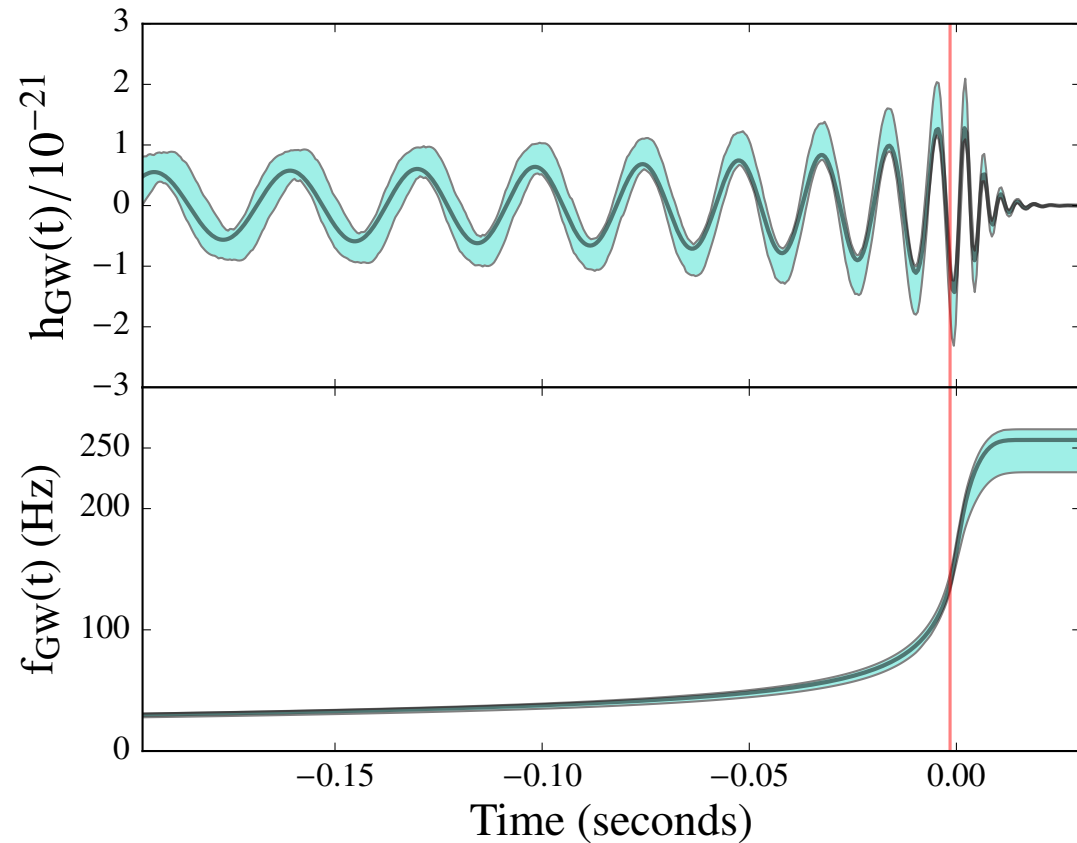
Tests of GR with LIGO's sources

- Given **current tight constraints** on GR (e.g., Solar system, binary pulsars), can **any GR deviation be observed with LIGO?**

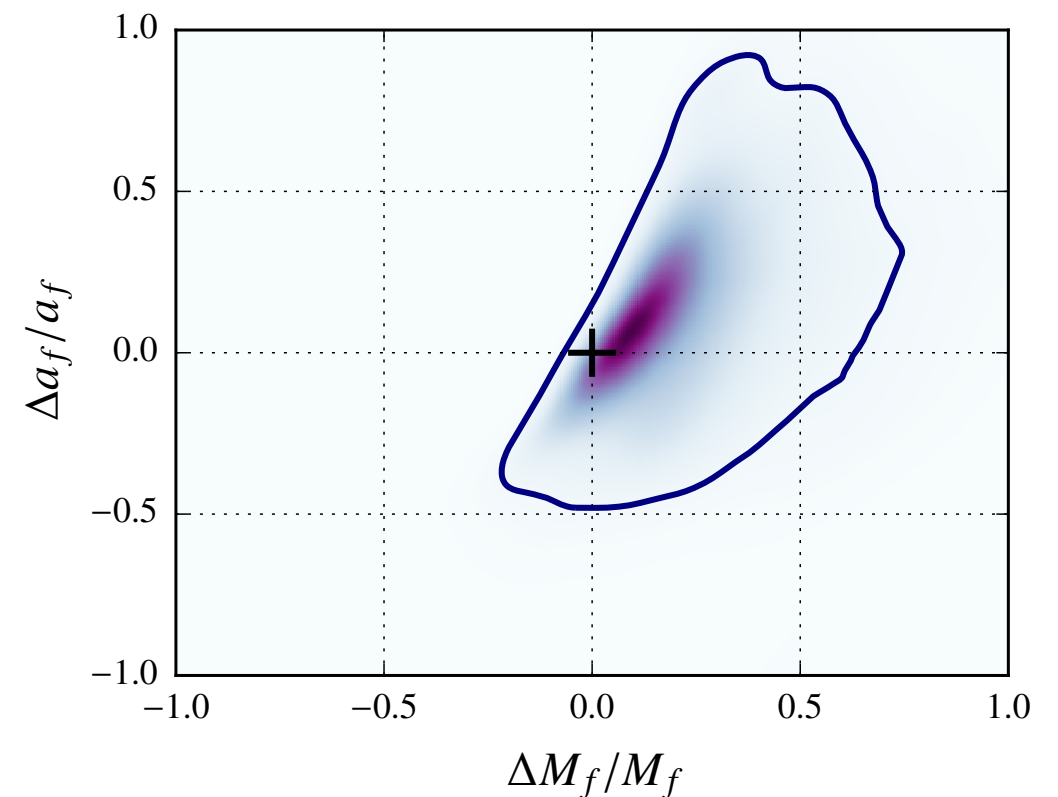


(credit: Sennett)

Inspiral-merger-ringdown consistency test



- Does **GW150914 deviate** from binary **black-hole predictions** in GR?
- We **compare final mass and spin estimates from inspiral and post-inspiral.**
- **No evidence of discrepancy from GR.**

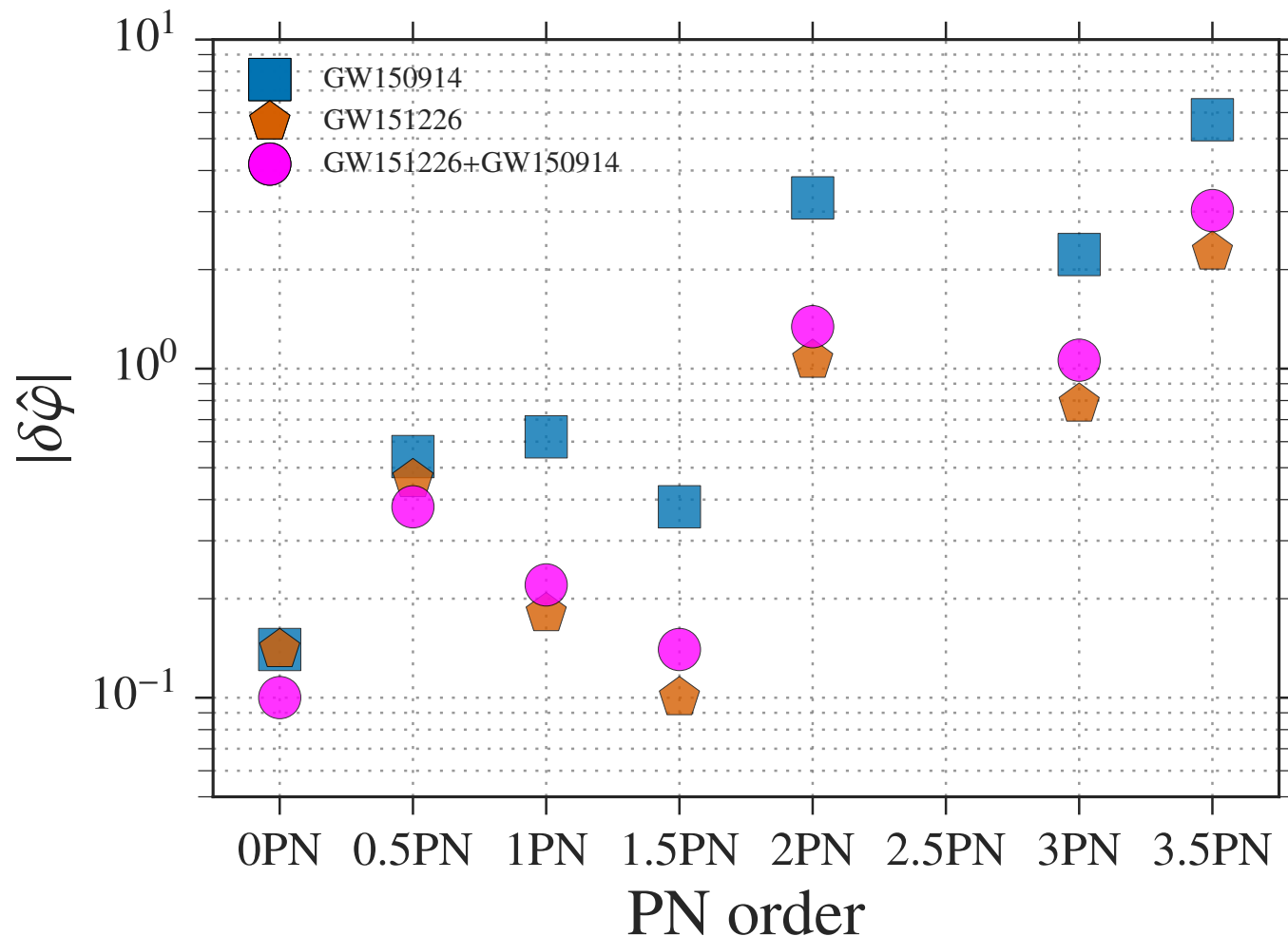


Tests of GR with LIGO's BHs: inspiral

- GW150914/GW122615's **rapidly varying orbital periods** allow us to **bound higher-order PN coefficients** in gravitational phase.

$$\tilde{h}(f) = \mathcal{A}(f)e^{i\varphi(f)} \quad \varphi(f) = \varphi_{\text{ref}} + 2\pi f t_{\text{ref}} + \varphi_{\text{Newt}}(Mf)^{-5/3} + \varphi_{0.5\text{PN}}(Mf)^{-4/3} + \varphi_{1\text{PN}}(Mf)^{-1} + \varphi_{1.5\text{PN}}(Mf)^{-2/3} + \dots$$

(Abbott et al. arXiv:1606.04856)

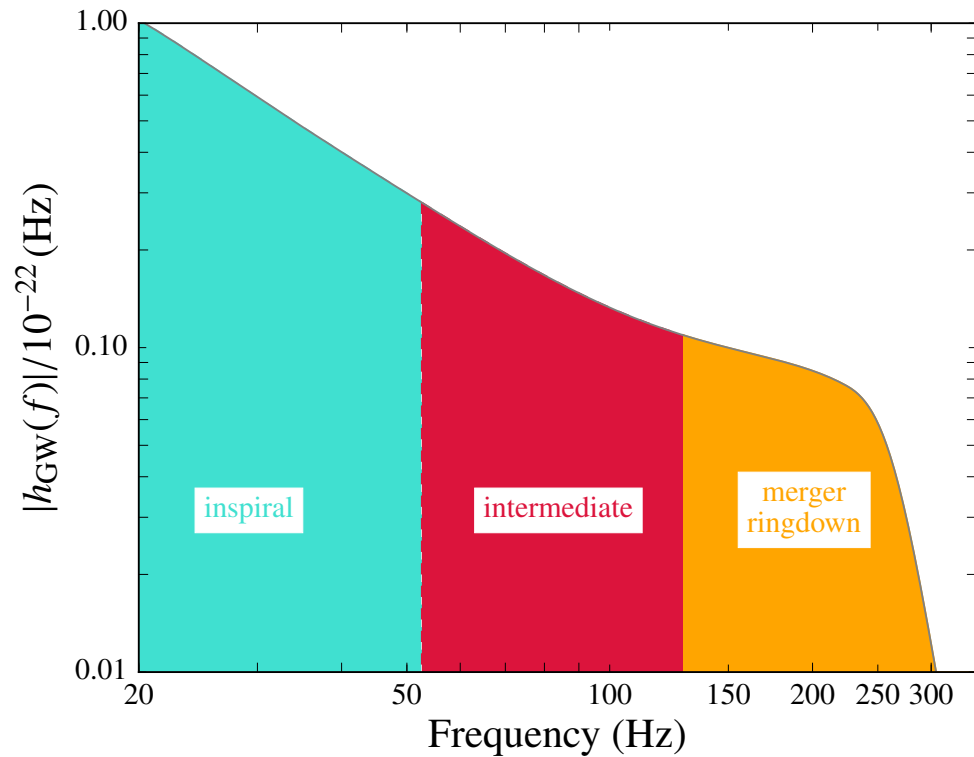


(Arun et al. 06 , Mishra et al. 10, Yunes & Pretorius 09, Li et al. 12)

- PN parameters** describe: **tails** of radiation due to backscattering, **spin-orbit** and **spin-spin** couplings.
- First **GR test** in the genuinely dynamical, **strong-field regime**.

Tests of GR with LIGO's BHs: late-inspiral-merger-RD

(Abbott et al. arXiv:1602.03841)



$$\begin{aligned} \varphi(f) = & \varphi_{\text{ref}} + 2\pi f t_{\text{ref}} + \varphi_{\text{Newt}} (Mf)^{-5/3} \\ & + \varphi_{0.5\text{PN}} (Mf)^{-4/3} + \varphi_{1\text{PN}} (Mf)^{-1} \\ & + \varphi_{1.5\text{PN}} (Mf)^{-2/3} + \dots + \beta_2 \log(Mf) \\ & + \dots + \alpha_4 \tan^{-1}(aMf + b) \end{aligned}$$

(Khan et al. 16)

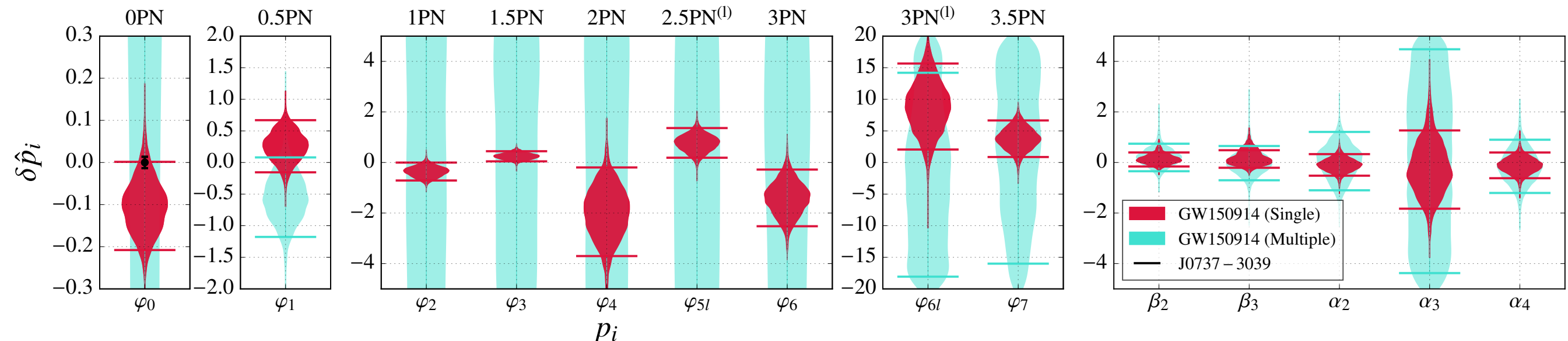
- Merger-ringdown **phenomenological parameters** (β_i and α_i) not yet **expressed in terms of relevant parameters in GR and modified theories of GR.**

(Yunes & Pretorius 09, Li et al. 12)

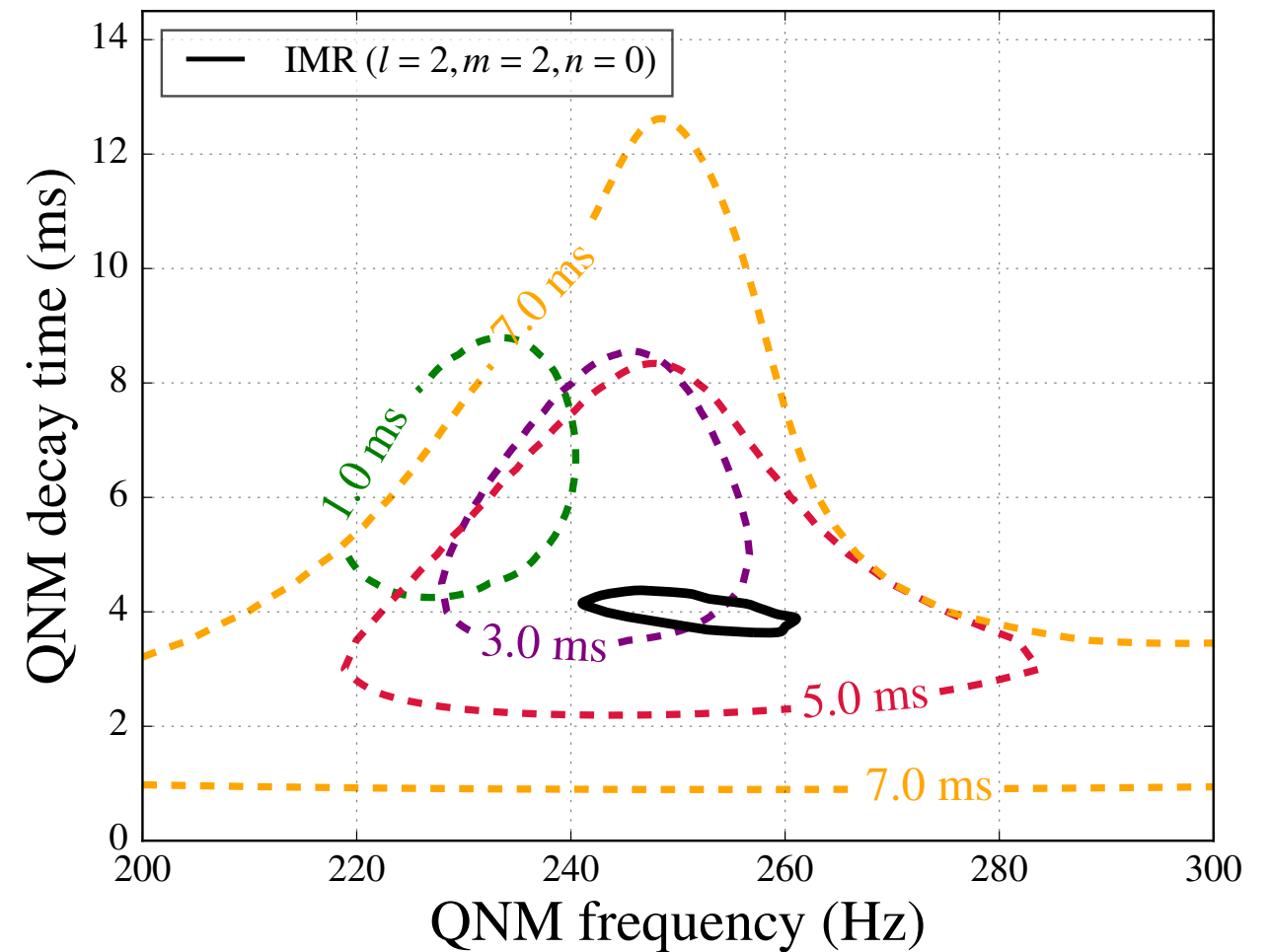
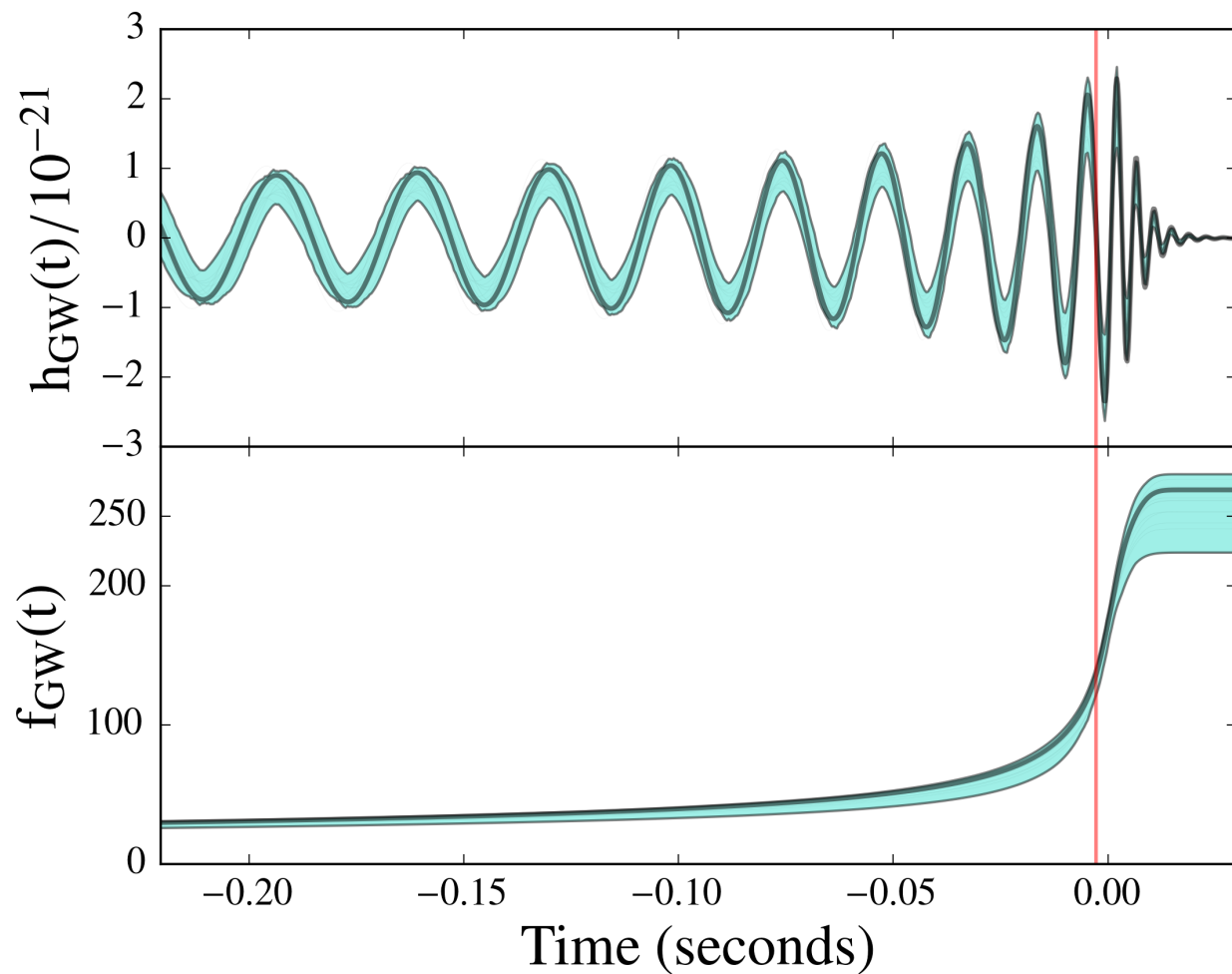
low frequency



high frequency



Could we prove that GW150914's remnant is a BH?



(Abbott et al. PRL 116 (2016) 221101)

- We measured frequency & decay time of **damped sinusoid** in the data after GW150914's peak.
- **Multiple QNMs** need to be measured to extract mass and spin of remnant, test **no-hair theorem** and **second-law black-hole mechanics** (Israel 69, Carter 71; Hawking 71, Bardeen 73).

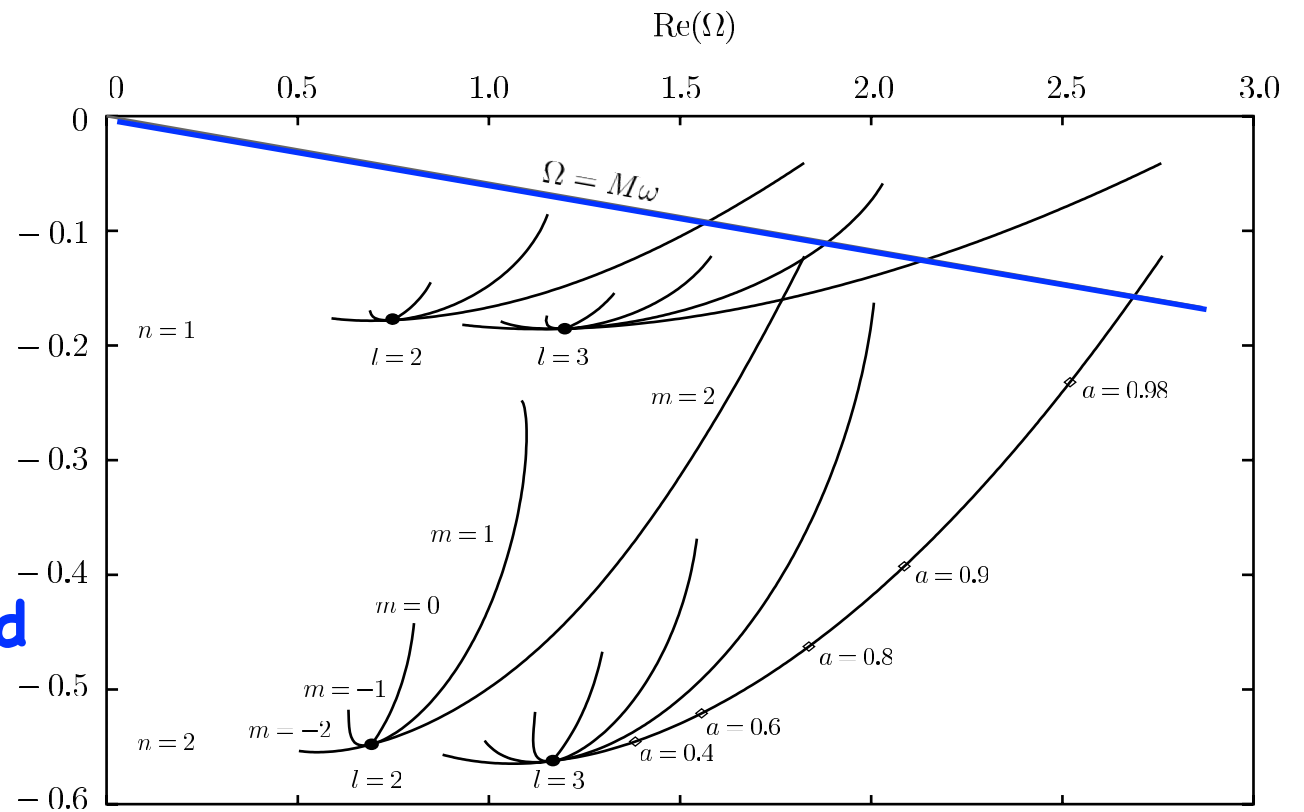
Measuring BH's mass and spin from multiple QNMs

$$\Omega_{nlm} = M\omega_{nlm}$$

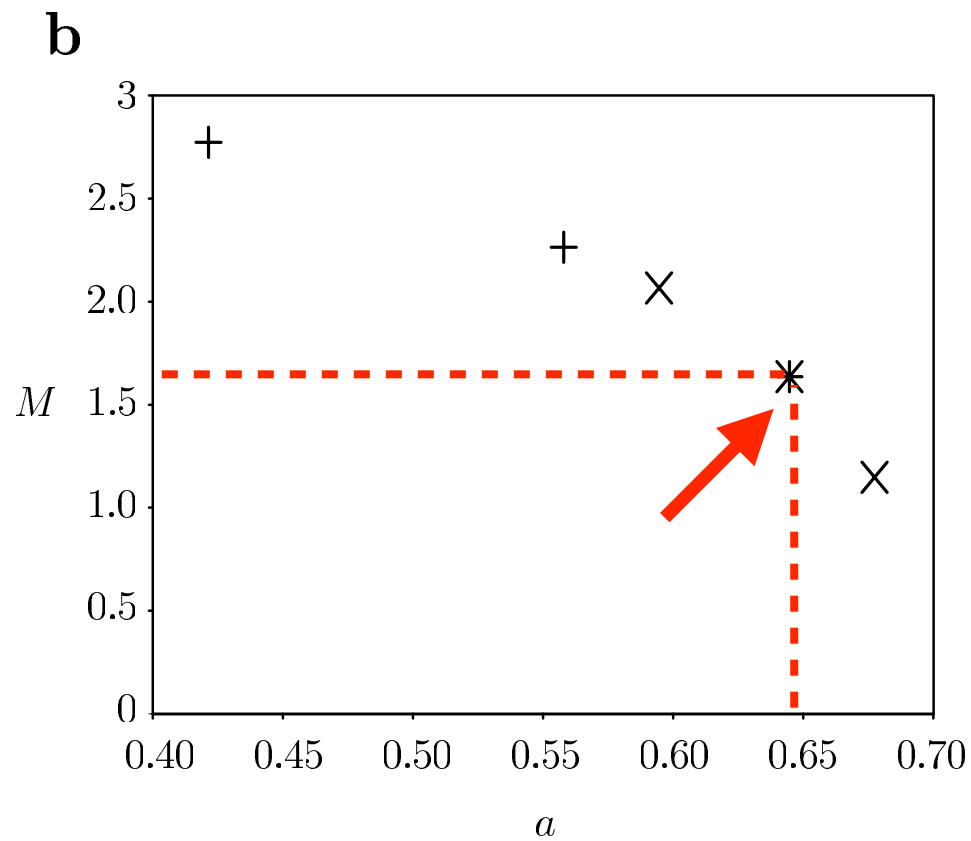
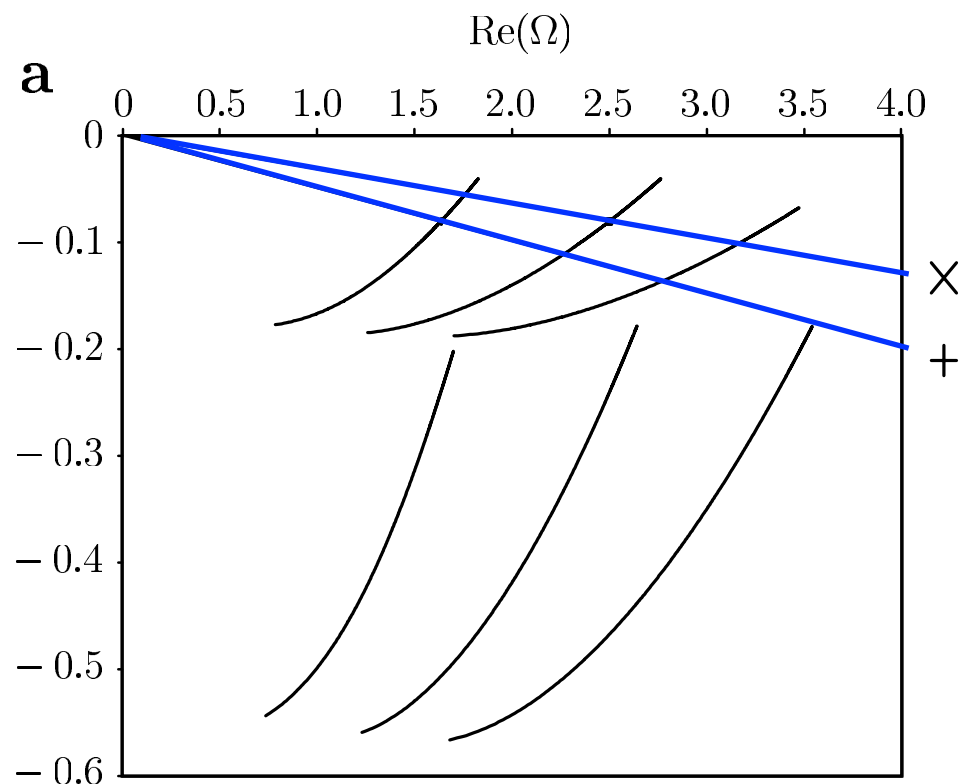
$$= \left(2\pi F_{nlm} + \frac{i}{T_{nlm}} \right)$$

Im(Ω)

- By knowing only **one frequency and decay time**, we cannot identify final BH's mass and spin.



(Dreyer et al. 03)



- To **measure multiple modes**, one needs either **high SNR** of $O(50-100)$ or **"stack"** many events.

Bounding the graviton Compton wavelength (mass)

- Phenomenological approach:

modified dispersion relation,

thus GWs travel at speed different from speed of light.

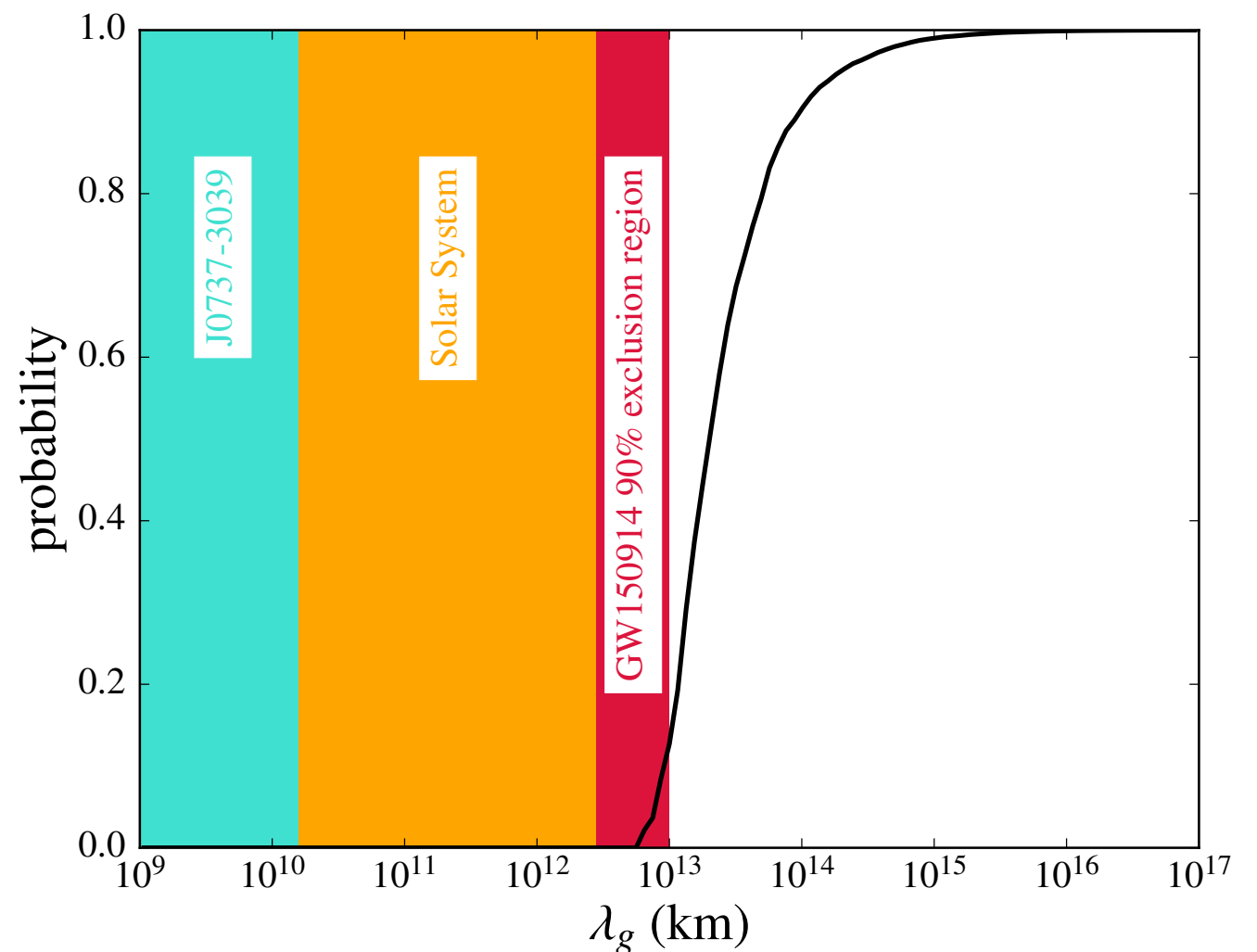
(Will 94)

$$E^2 = p^2 c^2 + m_g^2 c^4 \quad \lambda_g = \frac{h}{m_g c}$$

- Lower** frequencies **propagate slower than higher** frequencies.

$$\frac{v_g^2}{c^2} = 1 - \frac{h^2 c^2}{\lambda_g^2 E^2} \quad \longrightarrow \quad \varphi_{\text{MG}} = -\frac{\pi D c}{\lambda_g^2 (1+z) f} \quad m_g \leq 1.2 \times 10^{-22} \text{eV}/c^2$$

(Abbott et al. arXiv:1602.03841)

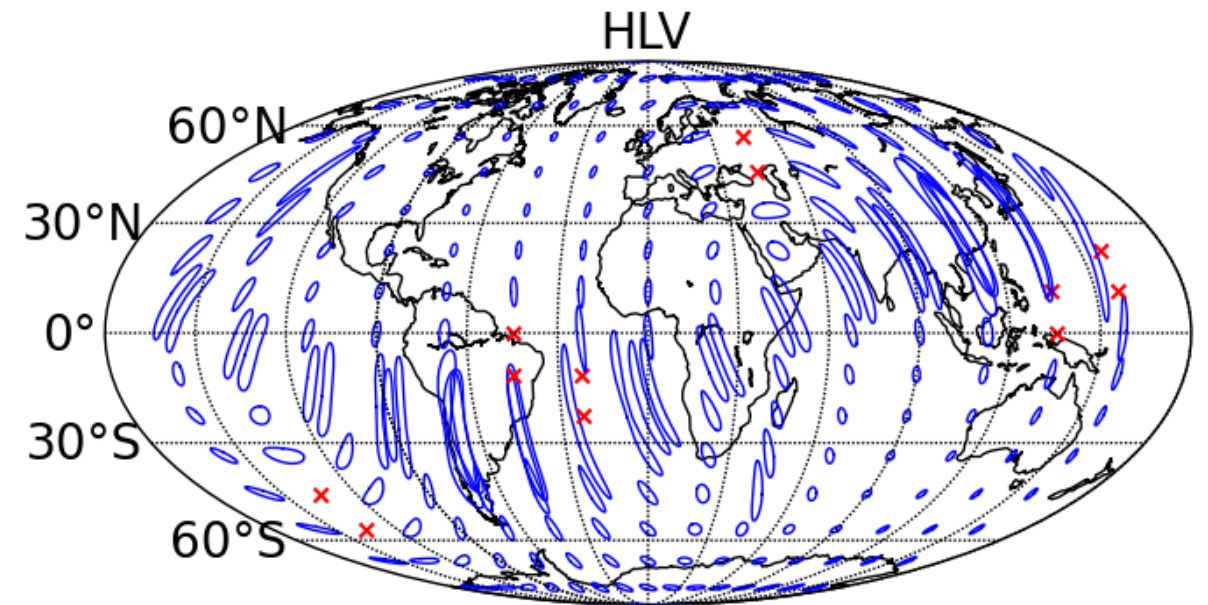
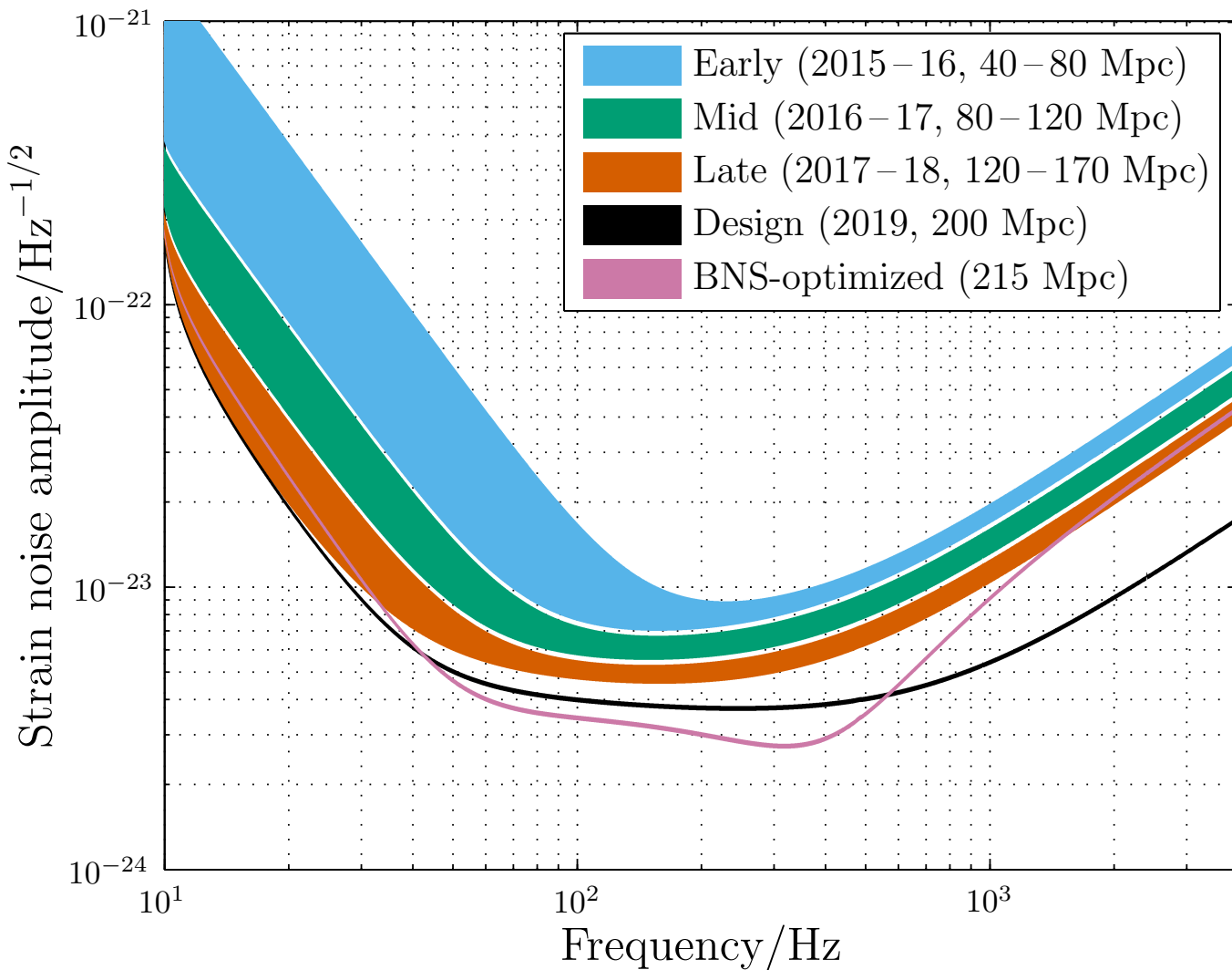


(see Yunes et al 16. for constraints on other dispersion relations, super- and sub-luminal GW propagation, Lorentz violation)

Advanced detectors' roadmap and sky localization

(Aasi et al. arXiv:1304.0670)

Advanced LIGO



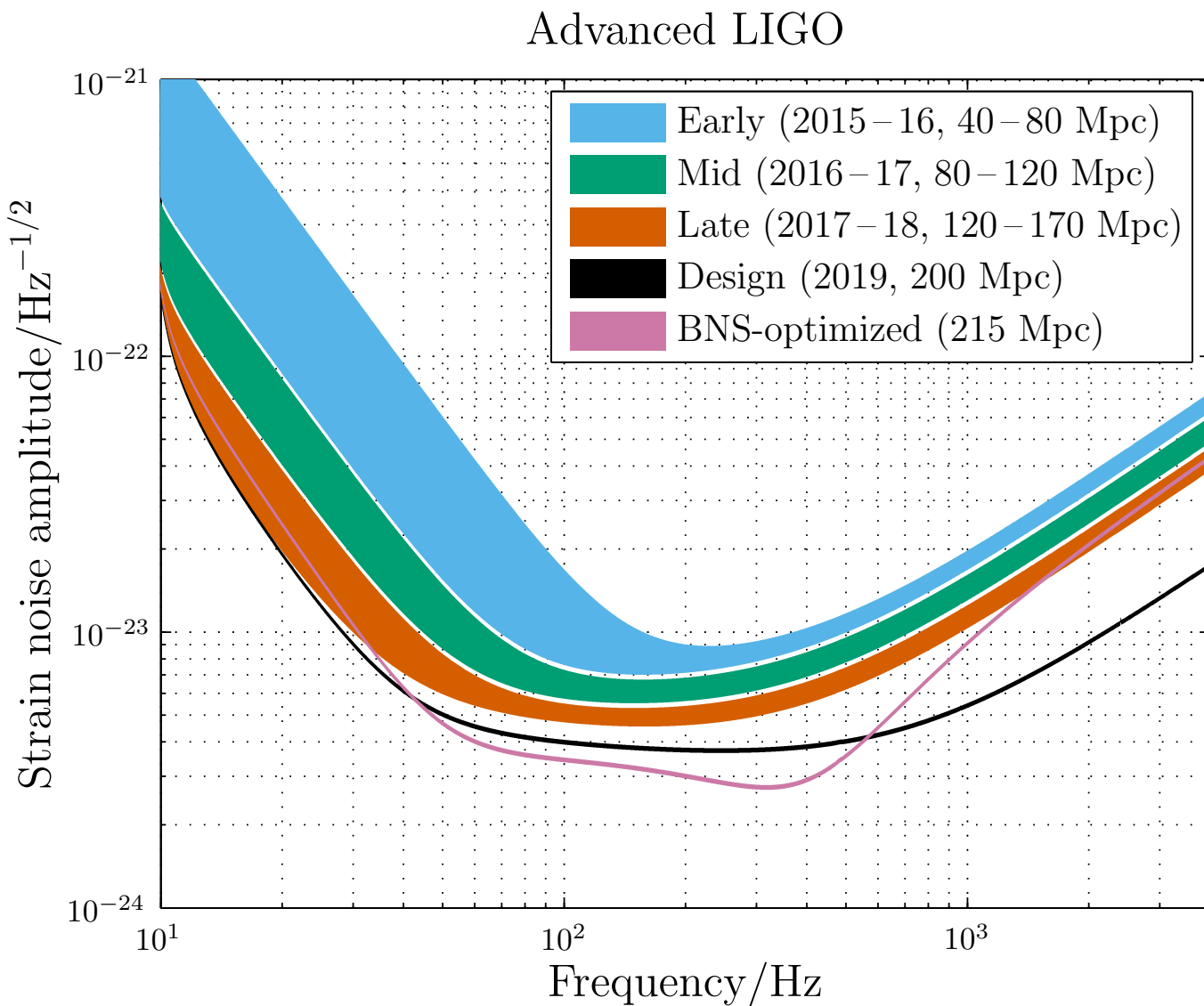
- Few **tens or hundred** square degrees

Detection rates @ **design sensitivity**:

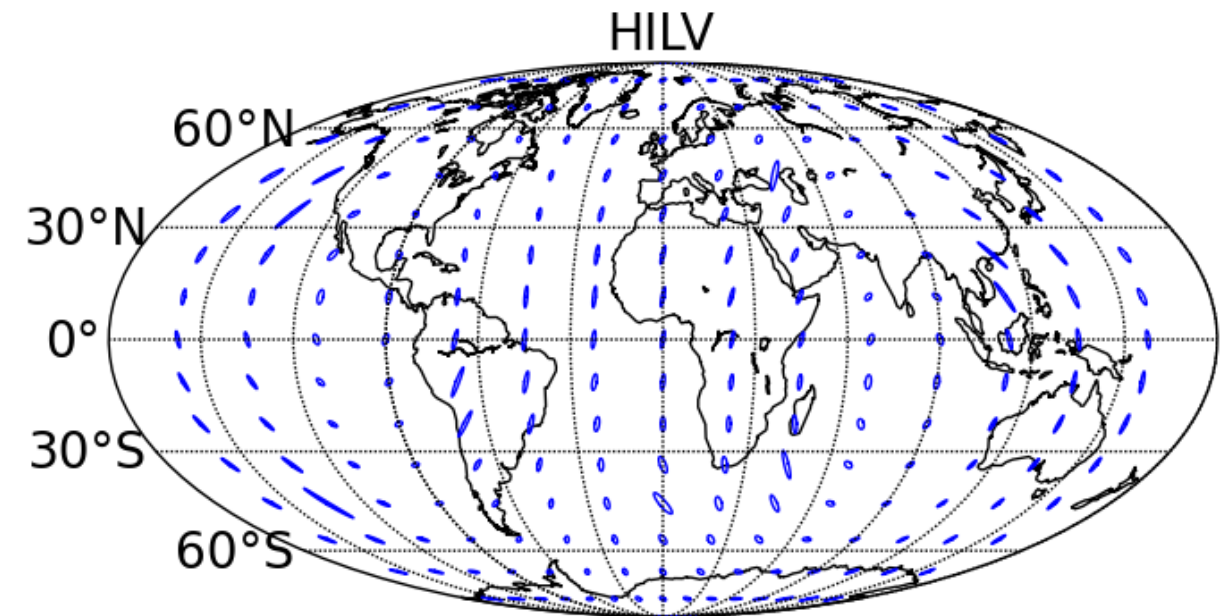
- **Binary neutron stars: 0.2 - 200 per year**
- **Binary black holes: tens to hundreds per year!**

Advanced detectors' roadmap and sky localization

(Aasi et al. arXiv:1304.0670)



with LIGO-India



- **Few** square degrees!

Detection rates @ **design sensitivity**:

- **Binary neutron stars: 0.2 – 200 per year**
- **Binary black holes: tens to hundreds per year!**